

NASA/CR-2017-219653



# Commercial Cargo Derivative Study of the Advanced Hybrid Wing Body Configuration with Over-Wing Engine Nacelles

*John R. Hooker, Andrew T. Wick, and Christopher J. Hardin  
Lockheed Martin Aeronautics Company, Marietta, Georgia*

---

November 2017

## NASA STI Program . . . in Profile

Since its founding, NASA has been dedicated to the advancement of aeronautics and space science. The NASA scientific and technical information (STI) program plays a key part in helping NASA maintain this important role.

The NASA STI program operates under the auspices of the Agency Chief Information Officer. It collects, organizes, provides for archiving, and disseminates NASA's STI. The NASA STI program provides access to the NTRS Registered and its public interface, the NASA Technical Reports Server, thus providing one of the largest collections of aeronautical and space science STI in the world. Results are published in both non-NASA channels and by NASA in the NASA STI Report Series, which includes the following report types:

- **TECHNICAL PUBLICATION.** Reports of completed research or a major significant phase of research that present the results of NASA Programs and include extensive data or theoretical analysis. Includes compilations of significant scientific and technical data and information deemed to be of continuing reference value. NASA counter-part of peer-reviewed formal professional papers but has less stringent limitations on manuscript length and extent of graphic presentations.
- **TECHNICAL MEMORANDUM.** Scientific and technical findings that are preliminary or of specialized interest, e.g., quick release reports, working papers, and bibliographies that contain minimal annotation. Does not contain extensive analysis.
- **CONTRACTOR REPORT.** Scientific and technical findings by NASA-sponsored contractors and grantees.

- **CONFERENCE PUBLICATION.** Collected papers from scientific and technical conferences, symposia, seminars, or other meetings sponsored or co-sponsored by NASA.
- **SPECIAL PUBLICATION.** Scientific, technical, or historical information from NASA programs, projects, and missions, often concerned with subjects having substantial public interest.
- **TECHNICAL TRANSLATION.** English-language translations of foreign scientific and technical material pertinent to NASA's mission.

Specialized services also include organizing and publishing research results, distributing specialized research announcements and feeds, providing information desk and personal search support, and enabling data exchange services.

For more information about the NASA STI program, see the following:

- Access the NASA STI program home page at <http://www.sti.nasa.gov>
- E-mail your question to [help@sti.nasa.gov](mailto:help@sti.nasa.gov)
- Phone the NASA STI Information Desk at 757-864-9658
- Write to:  
NASA STI Information Desk  
Mail Stop 148  
NASA Langley Research Center  
Hampton, VA 23681-2199

NASA/CR-2017-219653



# Commercial Cargo Derivative Study of the Advanced Hybrid Wing Body Configuration with Over-Wing Engine Nacelles

*John R. Hooker, Andrew T. Wick, and Christopher J. Hardin  
Lockheed Martin Aeronautics Company, Marietta, Georgia*

National Aeronautics and  
Space Administration

Langley Research Center  
Hampton, Virginia 23681-2199

Prepared for Langley Research Center  
under Contract NNL10AA06B/NNL15AB18T

November 2017

The use of trademarks or names of manufacturers in this report is for accurate reporting and does not constitute an official endorsement, either expressed or implied, of such products or manufacturers by the National Aeronautics and Space Administration.

Available from:

NASA STI Program/Mail Stop 148  
NASA Langlet Research Center  
Hampton, Virginia 23681-2199  
Fax: 757-864-6500



## TABLE OF CONTENTS

<b>List of Figures</b> .....	<b>2</b>
<b>Acronym List</b> .....	<b>3</b>
<b>Symbol List</b> .....	<b>4</b>
<b>I. Executive Summary</b> .....	<b>5</b>
<b>II. Introduction</b> .....	<b>5</b>
<b>III. Program Objectives</b> .....	<b>5</b>
<b>IV. Technical Approach</b> .....	<b>6</b>
Rapid Conceptual Design Process.....	6
CFD Based Analysis and Design Tools.....	6
Baseline Aircraft Mission Requirements.....	7
<b>V. Summary of Results</b> .....	<b>8</b>
B777 Sized Conventional Freighter.....	8
B757 Sized HWB Freighter.....	13
B777 Sized HWB Freighter.....	21
Summary of Results from Configuration Design Studies.....	26
Market Study Results Summary.....	32
Technology Maturation Roadmap.....	34
<b>VI. Conclusions</b> .....	<b>36</b>
<b>REFERENCES</b> .....	<b>37</b>

## List of Figures

<u>Figure</u>	<u>Page</u>
Figure 1: RCD Design Environment.....	6
Figure 2: Boeing 777F Twin-Aisle Derived Commercial Freighter (Boeing, 2016). .....	7
Figure 3: Boeing 757PF Twin-Aisle Derived Commercial Freighter (Boeing, 2007). .....	7
Figure 4: General Arrangement Drawing for the Conventional Tube-and-Wing B777 Sized Freighter. ....	9
Figure 5: Advanced Tube-and-Wing B777 Sized Freighter CFD Modeling Overview. ....	10
Figure 6: KNOPTER Based Optimization Results on the Advanced Tube-and-Wing Conventional B777 Freighter Configuration. ....	11
Figure 7: Pre-and Post Optimization Aerodynamic Performance Comparisons. ....	11
Figure 8: Performance and Stability and Control Characteristics of the Advanced Tube-and-Wing Conventional B777 Freighter Configuration.....	12
Figure 9: Range-Payload Comparison between the Conventional B777 Freighter Configuration and the Baseline 777F Configuration. ....	13
Figure 10: Comparison of HWB Fuselage Cross Section with Tube-and-Wing Design. ....	14
Figure 11: Two Options for HWB Main Deck ULD.....	14
Figure 12: Unit Load Device Selection. ....	15

Figure 13: CATIA based Parametric Surface Loft of the HWB Sized 757 Freighter. ....	15
Figure 14: General Arrangement Drawing for the HWB B757F Sized Freighter. ....	16
Figure 15: HWB 757 Cargo Bay Configuration. ....	17
Figure 16: Side Door Loading of AAX Container. ....	17
Figure 17: 757PF-Sized HWB Freighter Cargo Door. ....	18
Figure 18: Results from HWB 757 Engine Placement Study. ....	18
Figure 19: KNOPTER Based Optimization Results on the HWB 757 Freighter Configuration. ....	19
Figure 20: Pre-and Post Optimization HWB 757 Aerodynamic Performance Comparisons. ....	20
Figure 21: NASA HWB 757 Freighter Payload-Range. ....	20
Figure 22: Two ULD Types Selected for HWB 777 Cargo Bay. ....	21
Figure 23: Cargo Bay Section View with AMX and AYY ULDs. ....	22
Figure 24: Planform View of Final Cargo Bay Configuration Layout (29 AYY + 22 AMX). ....	22
Figure 25: Parametric CATIA Model for the 777F Sized HWB Freighter. ....	23
Figure 26: General Arrangement Drawing for the HWB 777 Sized Freighter. ....	23
Figure 27: HWB 777 Cargo Floor Arrangement. ....	24
Figure 28: HWB 777 Aerodynamic Optimization Results. ....	25
Figure 29: HWB 777 Final Aerodynamic Performance. ....	25
Figure 30: NASA HWB 777 Freighter Payload-Range. ....	26
Figure 31: Summary of Key Performance Characteristics of the Three Configurations Developed as Part of this Study. ....	27
Figure 32: Summary of Aerodynamic Performance Characteristics of the Three Configurations Developed as Part of this Study. ....	27
Figure 33: Aerodynamic Performance Comparisons between Configurations Developed for this Study and Existing Aircraft. ....	28
Figure 34: HWB Scalability Comparison. ....	29
Figure 35: Semi-Circular Fuselage Cross Sectional Shape for the HWB. ....	29
Figure 36: Increased Inboard Wing Thickness Study Results. ....	30
Figure 37: Aft Fuselage Study Results. ....	31
Figure 38: Yehudi Study Results. ....	31
Figure 39: Over-Wing Nacelle Benefits. ....	32
Figure 40: HWB Market Size Assessment. ....	33
Figure 41: HWB Commercial Freighter Market Assessment. ....	33
Figure 42: RCEE Program Based Highest Pay-Off Fuel Saving Technologies for Maturation. ....	34
Figure 43: Recommended Technology Maturation Roadmap. ....	35
Figure 44: Estimated Extent and Benefit of Natural Laminar Flow on the HWB. ....	36

## Acronym List

AATT	Advanced Air Transport Technology
AC	Aircraft
AFRL	Air Force Research Laboratory
CDISC	Constrained Direct Iterative Surface Curvature
CFD	Computational Fluid Dynamics
CFL	Courant–Friedrichs–Lewy
CG	Center of Gravity

DATCOM	Data Compendium
DOE	Design of Experiments
DP	Distributed Propulsion
EIS	Entry Into Service
ERA	Environmentally Responsible Aviation
ESF	Engine Scale Factor
FOD	Foreign Object Damage
HWB	Hybrid Wing Body
IOC	Initial Operating Capability
KNOPTER	Knowledge Based Optimizer
LaRC	Langley Research Center
LM	Lockheed Martin
MDAO	Multidisciplinary Design and Optimization
MTOW	Maximum Takeoff Weight
MZFW	Maximum Zero Fuel Weight
NASA	National Aeronautics and Space Administration
NLF	Natural Laminar Flow
N-S	Navier-Stokes
NTF	National Transonic Facility
OEM	Original Equipment Manufacturer
OML	Outer Mold Line
OWE	Operating Weight Empty
OWN	Over-Wing Nacelle
RANS	Reynolds Averaged Navier-Stokes
RCD	Rapid Conceptual Design
RCEE	Revolutionary Configurations for Energy Efficiency
RR	Rolls-Royce
SFC	Specific Fuel Consumption
SUSIE	Simple Unstructured Inverse Engineering
TRL	Technology Readiness Level
ULD	Unit Load Device
UPS	United Parcel Service
USAF	United States Air Force

## Symbol List

BL	Butt Line
CD	Drag Coefficient
CL	Lift Coefficient
CM	Pitching Moment Coefficient
Cp	Pressure Coefficient
CT	Thrust Coefficient
FS	Fuselage Station
L/D	Lift / Drag
M	Mach Number
ML/D	Aerodynamic Efficiency (Mach * Lift / Drag)

## **I. Executive Summary**

Lockheed Martin (LM) has teamed with both the Air Force Research Laboratory (AFRL) and the National Aeronautics and Space Administration (NASA) to develop a new strategic airlifter called the Hybrid Wing Body (HWB) and validate its performance. The HWB is a next generation transport that promises to revolutionize air mobility through a combination of efficiency, affordability, and compatibility. Results from extensive low speed and transonic wind tunnel testing have confirmed its high efficiency – estimated to use between 51 and 73% less fuel than today’s commercial freighters and military airlifters. It was designed to be an affordable configuration that can be built today, without the need for lengthy and costly enabling technology maturation. Finally, it is a multirole configuration that can perform the same missions as today’s dedicated fleets of airlifters, tankers, and commercial freighters.

Although originally developed as an airlifter for the Air Force, the same characteristics that make it a great airlifter will also make it a great commercial freighter. The objective of this program is to assess the performance of the HWB as a commercial freighter. This includes development of two different size freighters (both a Boeing 777 and 757 class) to assess the scalability of the HWB concept and detailed performance comparisons with today’s existing freighter fleet and a comparable future fleet of the same technology level. Results documented in this report indicate that a HWB-based commercial freighter, using technology levels available at an Entry Into Service (EIS) date of 2030-2035, would use approximately 30 – 60% less fuel than today’s commercial freighters and ~7% less fuel than an advanced tube-and-wing configuration using the same technology levels. These fuel saving estimates are dependent on freighter size and mission range.

## **II. Introduction**

LM has leveraged its partnership with the AFRL and NASA on the advanced hybrid wing body concept to develop a commercial freighter that addresses the NASA Advanced Air Transport Technology (AATT) Project goals for improved efficiency beyond 2025. The current AFRL Revolutionary Configurations for Energy Efficiency (RCEE) program established the HWB configuration and technologies needed for military transports to achieve aerodynamic and fuel efficiencies well beyond the commercial industry’s most modern designs. This study builds upon that effort to develop a baseline commercial cargo aircraft and two HWB derivative commercial cargo aircraft to quantify the benefit of the HWB and establish a technology roadmap for further development.

## **III. Program Objectives**

There are four technical objectives for this study. The first objective is the development of a conceptual design of a 777-sized conventional tube-and-wing commercial air cargo freighter aircraft and quantification of the potential reductions in aircraft fuel consumption with technology consistent with an entry into service beyond 2025 (N+3 timeframe). The second objective is the development of two conceptual designs of an HWB-based commercial air cargo freighter aircraft (both Boeing 777 and 757 sized) and quantification of the potential reductions in aircraft fuel



a cell-centered finite-volume formulation with upwind flux differencing in the solver. For this study, steady-state Reynolds Averaged Navier-Stokes (RANS) simulations were performed with the one equation Spalart-Allmaras turbulence model. Wall functions were used to solve the boundary layer with a  $y^+$  of 50 used to predict the skin friction. Solutions were generally run between 6000 and 8000 iterations at a Courant–Friedrichs–Lewy (CFL) number of 100 to achieve acceptable convergence, which was defined as the point where lift, drag, and pitching moment residuals had dropped about three orders of magnitude. An angle-of-attack seeking algorithm was used in the solver in order to achieve a specified overall aircraft wing lift coefficient.

Aerodynamic shape optimization was a critical enabler for this effort as it was utilized to ensure a true assessment of the performance potential of HWB with Over-Wing Nacelle (OWN) concepts by minimizing adverse engine / wing interference effects. Critical requirements for the optimizer were rapid analysis times coupled with appropriate fidelity. LM has developed the KNOPTER (KNOWledge based OPTimizER) optimization process that builds upon two mature, knowledge-based design methods developed by NASA. These methods are the Constrained Direct Iterative Surface Curvature (CDISC) inverse design methodology and the Simple Unstructured Inverse Engineering (SUSIE) stationless design method (Reference 3). KNOPTER (described in References 4 - 6) permits drag-based shape optimization with these rapid knowledge-based design methods. It also provides the appropriate Navier-Stokes (N-S) CFD based fidelity for transonic cruise simulations (Reference 7).

### **Baseline Aircraft Mission Requirements**

The vehicles designed in this study are comparable in size and payload-range performance to either the 777F (a Boeing 777-200LR derived freighter depicted in Figure 2) or the 757PF (a Boeing 757-200 derived freighter depicted in Figure 3). Full details of the vehicle and mission requirements are detailed in the three configuration detailed design reports delivered as separate reports as part of this program.



**Figure 2: Boeing 777F Twin-Aisle Derived Commercial Freighter (Boeing, 2016).**



**Figure 3: Boeing 757PF Twin-Aisle Derived Commercial Freighter (Boeing, 2007).**

## V. Summary of Results

### B777 Sized Conventional Freighter

The objective of this task was the development of a conceptual aircraft design capable of replacing the Boeing 777-200LR derived freighter (777F) using an advanced tube-and-wing vehicle configuration arrangement and to understand the impact modern technology (advanced aerodynamic design tools, high bypass ratio engines, and advanced lightweight materials) has on mission performance. Technology levels applied are assumed to be available at an EIS date of 2030-2035. The resulting configuration is described in detail in the “Conventional Commercial Cargo Design Report” delivered as part of this effort. The following provides an overview of the advanced tube-and-wing B777 sized freighter development.

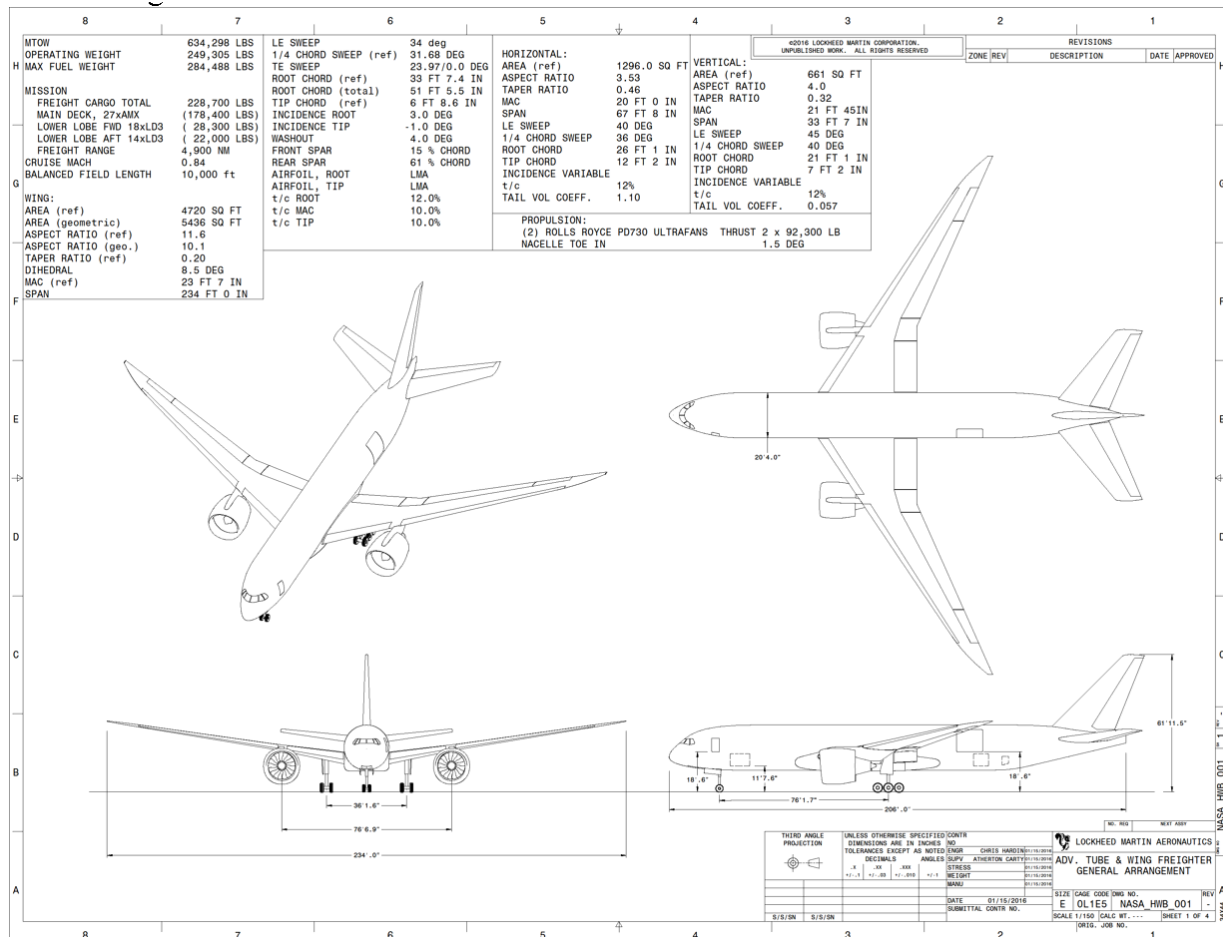
Initial cruise aerodynamic performance estimates were based on classical empirical methods. LM uses a combination of techniques from a variety of well-known sources: USAF DATCOM, Raymer, Roskam, Torenbeek and Nicolai. The compressibility drag rise portion of parasite drag attributed to the wing was calculated using Lockheed-California Company (CALAC) MD100 method. The method was developed at Lockheed in the later years of the L-1011 program for L-1011-500 (EIS 1979).

An estimation of top-level component weights was performed using proprietary LM methods within ASSET (LM’s computer software package for aircraft design, synthesis and mission performance). The methods are parametric and contain calibration coefficients that may be adjusted to match weights of a known vehicle. In this case, coefficients were adjusted prior to the study to closely match published Boeing 777F weights. This was accomplished by building a synthesis model (based on the 2011 NASA Environmentally Responsible Aviation (ERA) study) for the 777F. Here, LM used engine original equipment manufacturer (OEM) provided thrust and fuel flows for a GE90-115.

The vehicle in this study uses an advanced turbofan engine (Rolls-Royce (RR) UltraFan) made available to LM. Thrust and fuel flow as a function of Mach and altitude were provided. Three specified power tables were identified: takeoff power, climb power and continuous power. Baseline engine thrust was scaled using the term Engine Scaling Factor (ESF). Engine thrust specific fuel consumption (SFC) was assumed to remain constant as ESF varied. So fuel flows and thrusts were scaled together to obtain the same SFC, for the same combination of Mach, altitude and throttle setting as the baseline engine.

As described in detail in the “Conventional Commercial Cargo Design Report,” Phoenix Integration ModelCenter 11 was used to perform the sizing trade studies to determine the basic configuration characteristics. With sizing completed, a CATIA loft was produced. It contains outer mold line (OML) surface definitions including primary flight controls, a preliminary landing gear layout, an internal cargo arrangement and a flight deck. Using the volumetric centroids of these components in CATIA, a center of gravity (CG) excursion diagram was created to assess the extent of CG travel in relation to the landing gear and mean aerodynamic chord. Finally, landing gear and nacelle locations were iterated upon to satisfy the design constraints (gear load limits, tip-back angle, turnover angle, collapsed nose strut). A mild increase in wing dihedral (2.5 deg) was

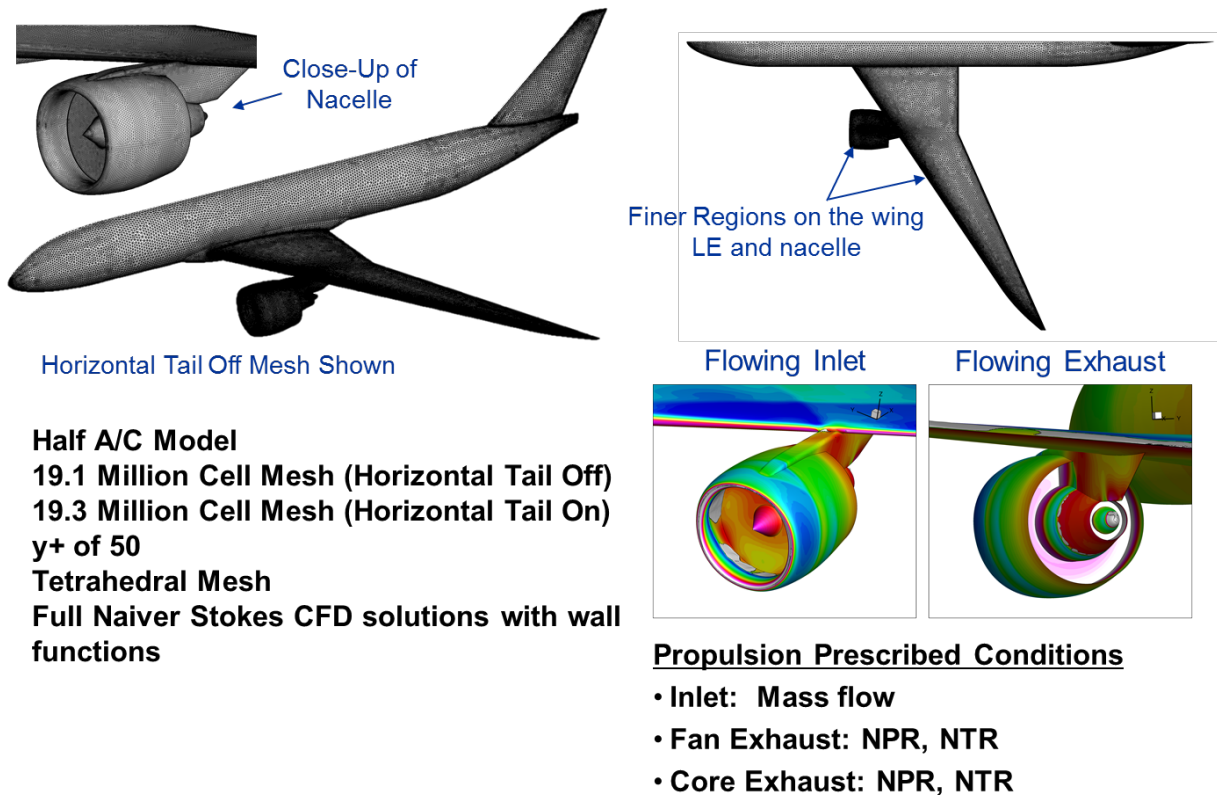
ultimately required to satisfy the main deck loading height requirement and to prevent the nacelle contact with the ground in the event of a collapsed nose gear strut. A general arrangement drawing for the resulting advanced tube-and-wing B777 sized commercial freighter is depicted in Figure 4.



**Figure 4: General Arrangement Drawing for the Conventional Tube-and-Wing B777 Sized Freighter.**

This is considered the baseline vehicle in this study and was developed for follow-on comparison with the advanced hybrid wing body design. It was configured using the conventional tube-and-wing approach. It consists of a fuselage with circular cross-section and a wing carry-through structure positioned below the main cargo floor. The empennage arrangement consists of a single vertical tail with lower mounted horizontal tail attached to aft fuselage sidewalls. Configuration selection follows the approach used during the NASA ERA study for the 1998 baseline and more advanced 2025 designs. Since the scope of this study was limited, a low wing design was retained throughout the effort despite difficulties integrating the large RR UltraFan engine having a 16 foot nacelle diameter. Long main landing gear were required to avoid nacelle contact with the ground in the event of a collapsed nose gear strut. At the same time, main gear length, which drives deck height, also effects loadability of the main cargo deck. It is desirable to use standard main deck loaders (218" to 220") which exist today for 777. So, the main gear must be long enough to avoid nacelle/ground contact if the nose gear collapses but short enough to permit main deck loading by typical loaders.

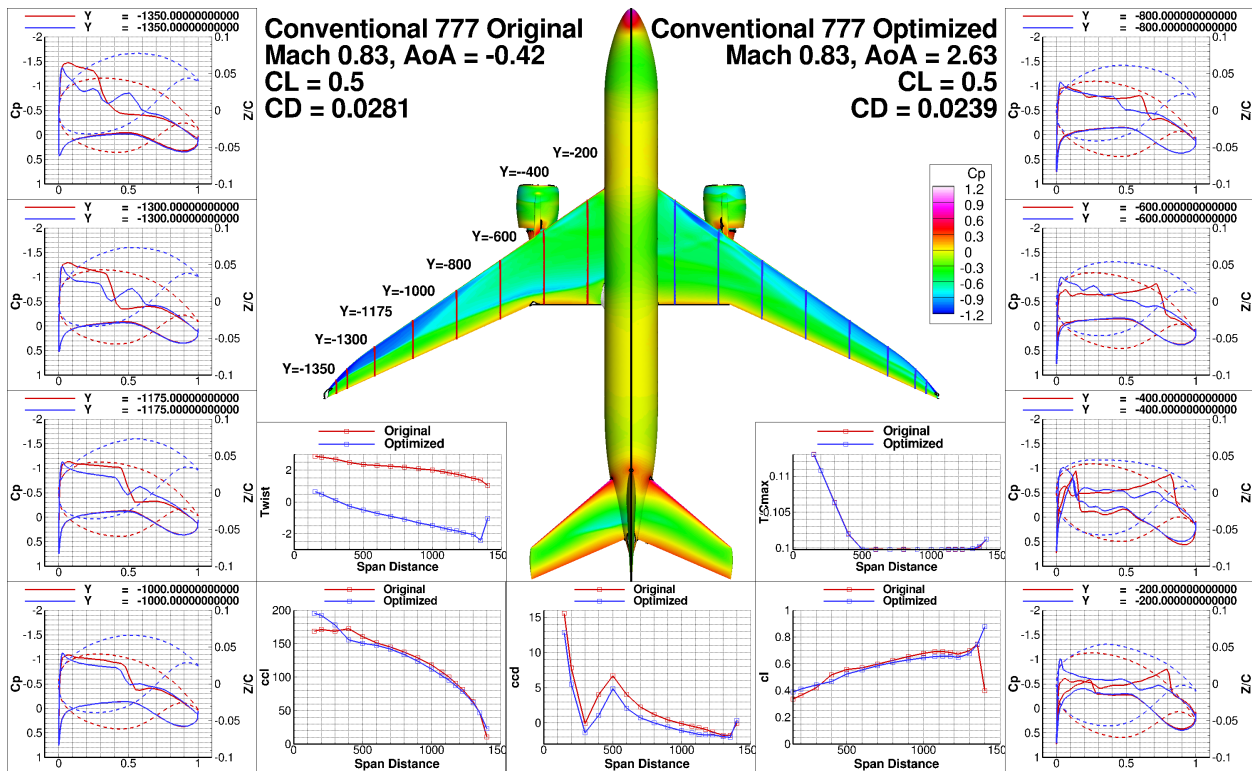




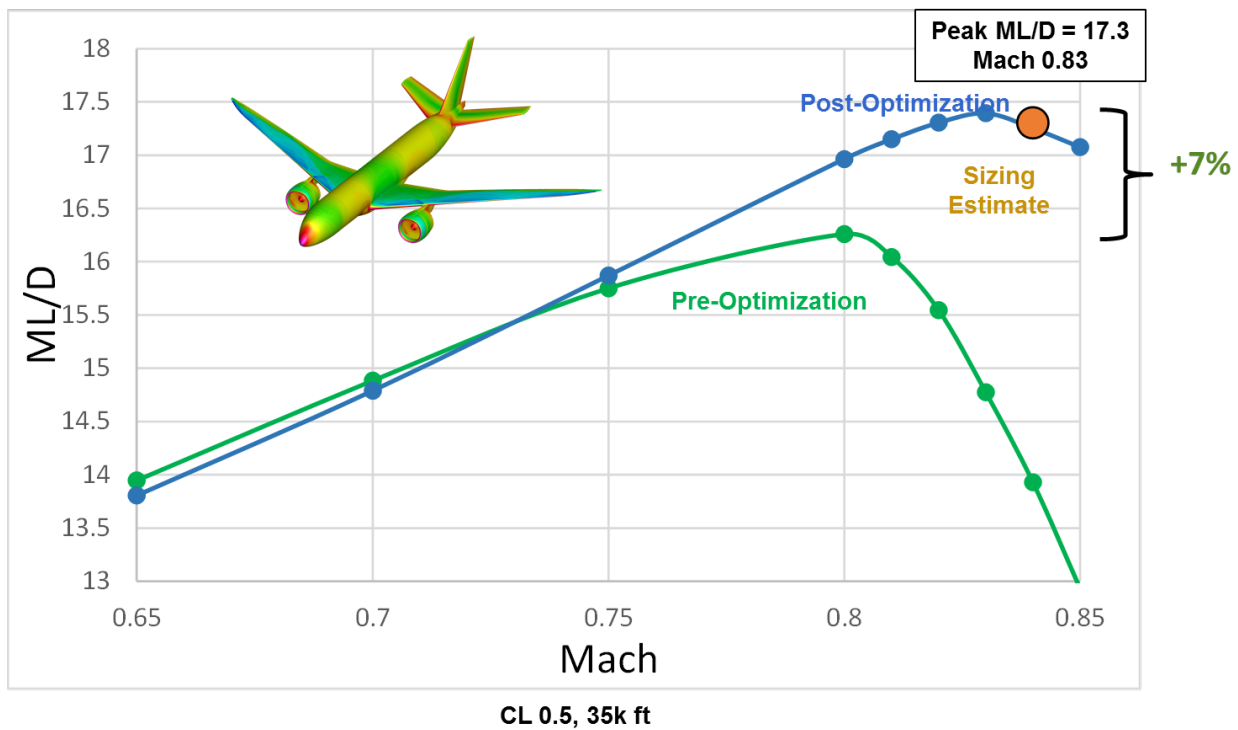
**Figure 5: Advanced Tube-and-Wing B777 Sized Freighter CFD Modeling Overview.**

With the loft of the configuration completed, detailed Navier-Stokes CFD based simulations were then performed. An overview of the CFD meshes and approach is depicted in Figure 5. This figure highlights the detail associated with the computational mesh. A typical half aircraft mesh used for this study contained approximately 19 million cells and utilized wall functions with a y+ of 50 to define the viscous boundary layer. Propulsive effects were simulated using a prescribed mass flow through the inlet and fan and core exhaust nozzle pressure and temperature ratios. This data was determined using the engine deck data obtained from Rolls-Royce for the UltraFan engine used in this study.

After the baseline CFD simulations were completed, KNOPTER was used to optimize the configuration for improved performance. A comparison of the baseline and optimized surface pressure distributions, airfoil shapes, wing span load, and wing twist is depicted in Figure 6. From this figure, it can be seen that the optimization significantly reduced the wing shock strength along the wing span and resulted in a 42 count drag reduction at cruise conditions (Mach=0.83, CL=0.5). The drag rise for both the baseline and optimized configurations is depicted in Figure 7 with aerodynamic efficiency (as measured with Mach \* Lift / Drag) plotted as a function of Mach number. This figure depicts the large improvement in performance (7%) associated with the KNOPTER optimization process, highlighting a peak ML/D of 17.3 is achieved at a cruise Mach of 0.83 (as indicated with peak aerodynamic efficiency). Also depicted in this figure is the estimated performance from the sizing effort with the lower fidelity aerodynamic estimation methods (shown with the orange circle).

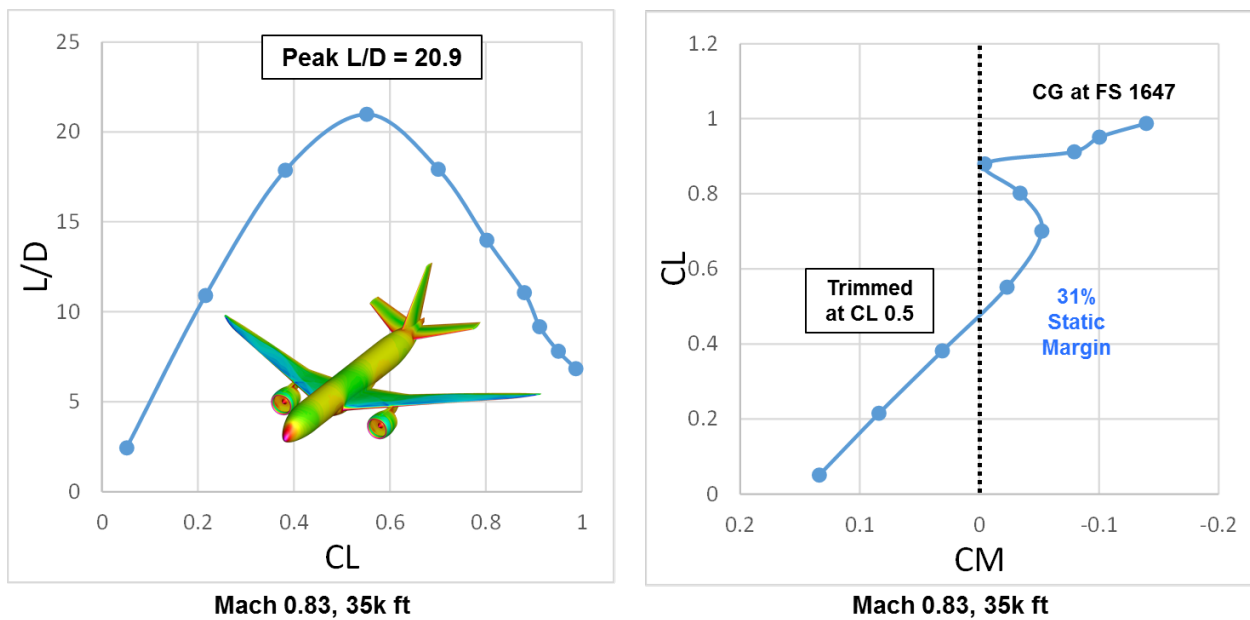


**Figure 6: KNOPTER Based Optimization Results on the Advanced Tube-and-Wing Conventional B777 Freighter Configuration.**

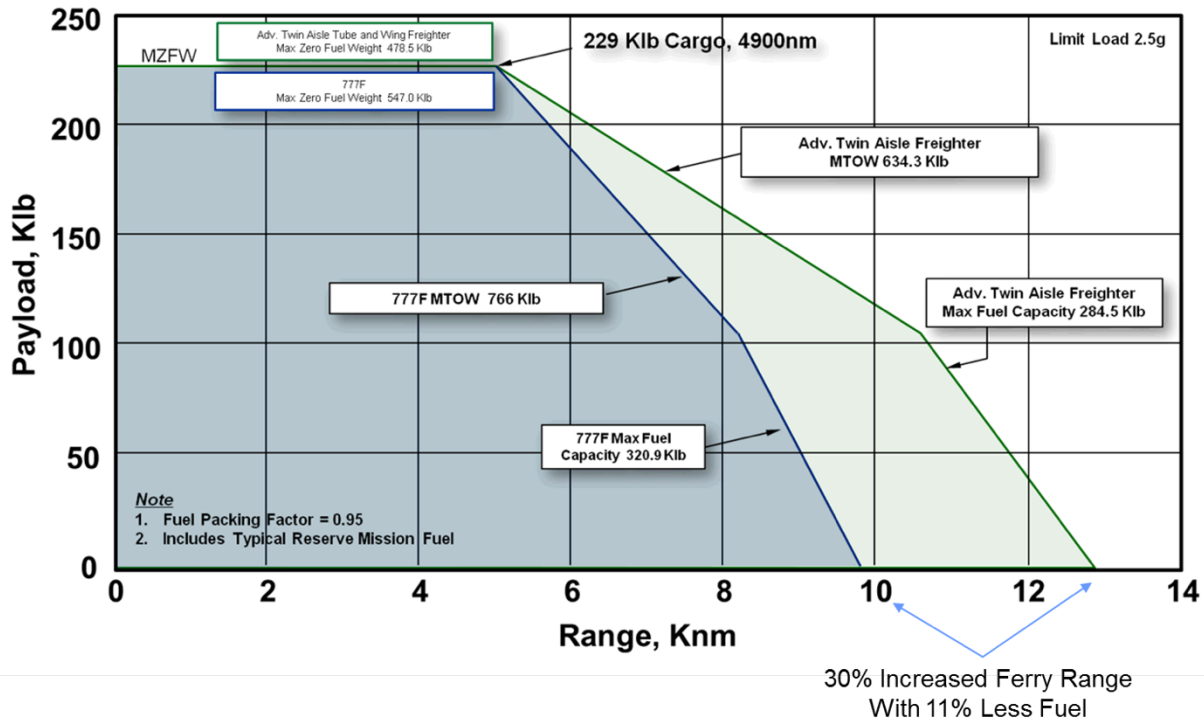


**Figure 7: Pre-and Post Optimization Aerodynamic Performance Comparisons.**

The performance and stability and control characteristics of the conventional B777 freighter configuration is depicted in Figure 8 with L/D plotted as a function of lift coefficient (CL) and lift coefficient (CL) plotted as a function of pitching moment (CM). Results from this figure indicate that a peak L/D is achieved at a CL of  $\sim 0.55$  and that the off-design performance of the configuration is robust as there is no rapid drop-off in performance as CL is changed. This figure also highlights a couple of interesting stability and control characteristics. For example, it highlights that the configuration is trimmed at the cruise lift coefficient of 0.5, minimizing trim drag. It also highlights an unstable pitch break at a lift coefficient of  $\sim 0.7$ . This is a characteristic of high aspect ratio swept wings and would typically be solved either with digital flight controls to tie elevator deflection with aircraft angle of attack or with vortex generators installed on the wing. Finally, a payload-range diagram (Figure 9) was created using the mission performance model and is compared with the 777F.



**Figure 8: Performance and Stability and Control Characteristics of the Advanced Tube-and-Wing Conventional B777 Freighter Configuration.**

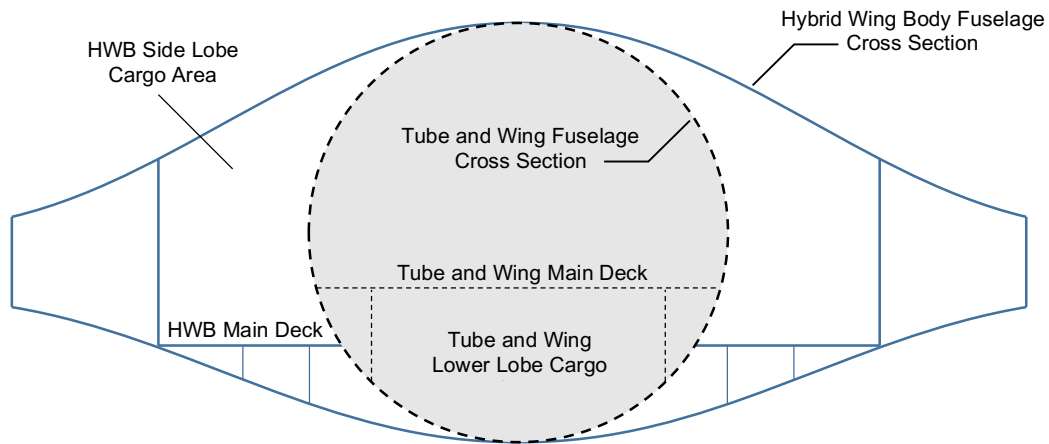


**Figure 9: Range-Payload Comparison between the Conventional B777 Freighter Configuration and the Baseline 777F Configuration.**

### B757 Sized HWB Freighter

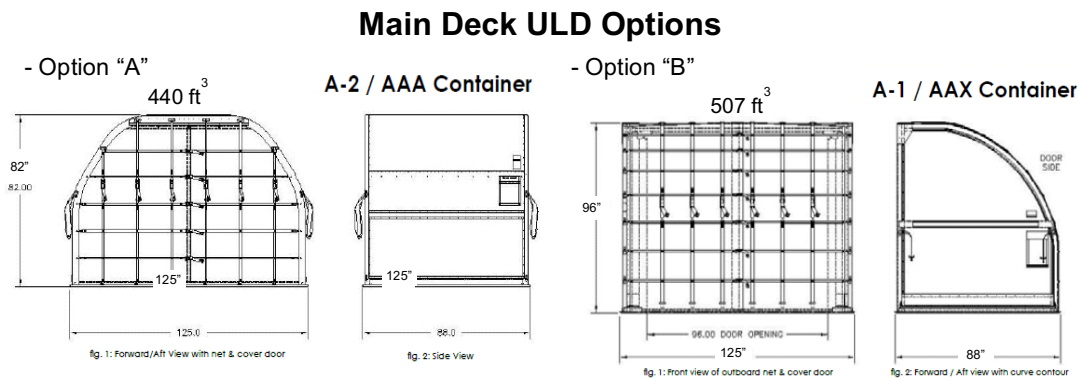
The objective of this task is the development of a conceptual aircraft design capable of replacing the Boeing 757-200 derived freighter (757-200PF) using a hybrid wing body (HWB) vehicle configuration arrangement and to understand the impact modern technology (innovative configuration shaping, advance aerodynamic design tools, high bypass ratio engines, and advanced lightweight materials) has on mission performance. Technology levels applied are assumed to be available at an EIS date of 2030-2035. The resulting configuration is described in detail in the “Advanced HWB Based 757F Replacement Design Report” delivered as part of this effort. The following provides an overview of the 757F sized HWB freighter development.

In order to predict vehicle performance, a loft of the vehicle OML was required to provide basic dimensions (wetted areas, lengths volumes, etc). Before starting the loft, a cargo bay definition, sized to the payload requirements, was needed. Here, a trade study was performed to determine the best cargo bay configuration for the HWB shape. Compared to a tube-and-wing, the HWB aircraft has more cross sectional area available for cargo in the spanwise direction as shown in Figure 10. In contrast, the tube-and-wing design has area available for cargo under the main deck. Current LM HWB designs feature a low cargo floor, typical of many existing air mobility assets. This feature prohibits storage of cargo under the HWB main deck floor. However, volume in this area remains available for systems.



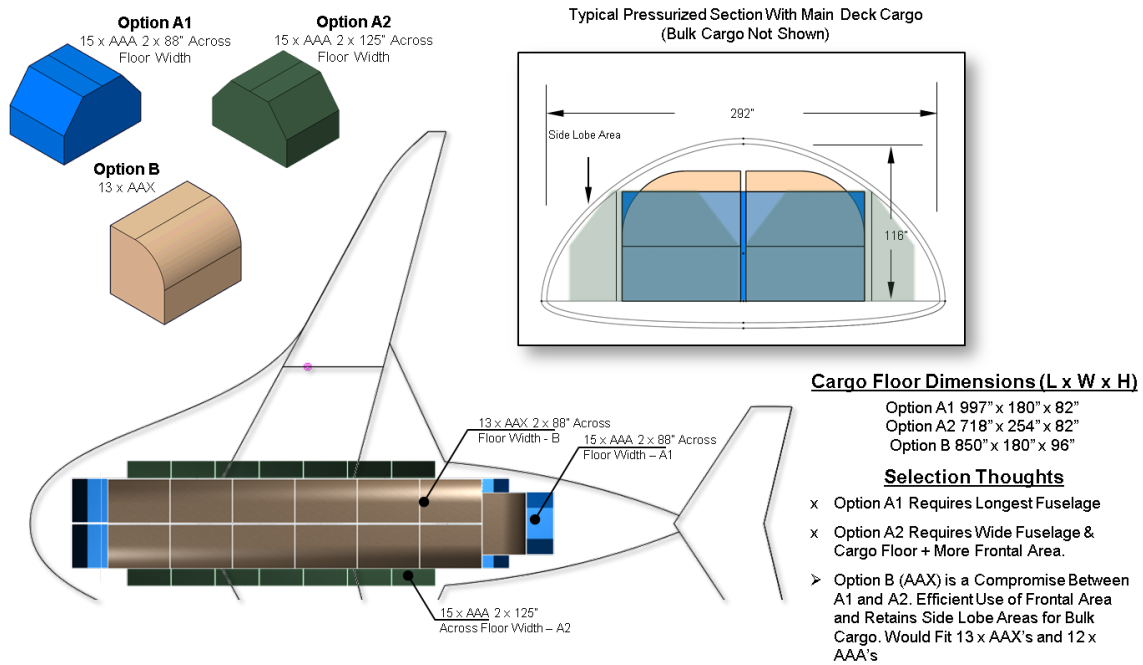
**Figure 10: Comparison of HWB Fuselage Cross Section with Tube-and-Wing Design.**

A survey of cargo container types was made to find shapes that best suit the HWB cross section characteristics. Two container types were downselected from the 13 main deck unit load device (ULD) types available in (Satco Inc., 2010): A-2 AAA (used by 757PF) and A-1 AAX as shown in Figure 11.

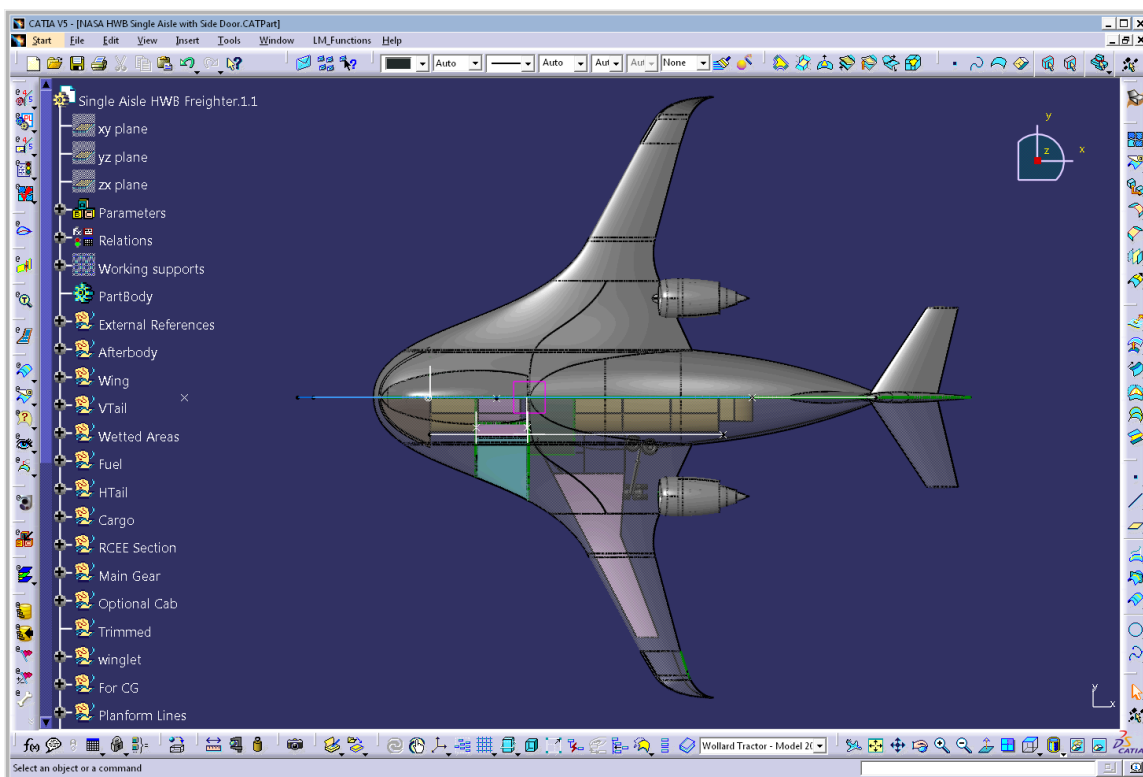


**Figure 11: Two Options for HWB Main Deck ULD.**

For the A-2 AAA container, two position options were evaluated (Figure 12): Option A1 positions the container's 88" edge across the cargo bay width while Option A2 position rotates the container 90 degrees. In each case (Option A1, Option A2), containers are positioned 2-abreast across the cargo floor to make best use of the available spanwise cross-sectional area. Option A1 required the longest cargo floor while retaining area in the side lobe for bulk cargo. Option A2 yielded the shortest and widest cargo floor footprint. It also required the use of volume in the side lobe. Option B (13 x AAX containers) is a compromise between the width and length of Option A1 and A2. It makes efficient use of the configurations frontal area while retaining area in the side lobe for bulk cargo. For this reason, cargo layout Option B was selected. The main deck cargo bundle measures 850" long, 180" wide and is 96" high. A fuselage cross section was lofted to match this width and height. See the inset in Figure 12.



**Figure 12: Unit Load Device Selection.**



**Figure 13: CATIA based Parametric Surface Loft of the HWB Sized 757 Freighter.**

With the cargo bay dimensions determined, a surface loft of the vehicle OML was created in CATIA (depicted in Figure 13). The loft is parametric and provides basic dimensional data used to predict cruise aerodynamic performance and component weights for analysis. Principal parameters (independent variables) are: wing area, aspect ratio, wing leading-edge sweep, wing taper ratio, wing average thickness, wing longitudinal position and engine scale factor. Tails were sized using historical volume coefficients, 0.057 for the vertical and 0.90 for the horizontal. Also, as changes are made to wing area, sweep or wing longitudinal position, tail areas automatically adjust to keep tail volumes constant.

As described in detail in the “Advanced HWB Based 757F Replacement Design Report,” a sizing study was performed to determine the optimum vehicle size. The OML surface loft was then updated to reflect the new characteristics. A general arrangement drawing of the optimized HWB freighter is depicted in Figure 14.

The final internal arrangement configured with 13 AAX unit load devices on the main cargo deck is depicted in Figure 15. 850” of deck length was required assuming a 2” spacing (fore-aft) between ULDs loaded 2 abreast with 4” spacing (left-right) on centerline.

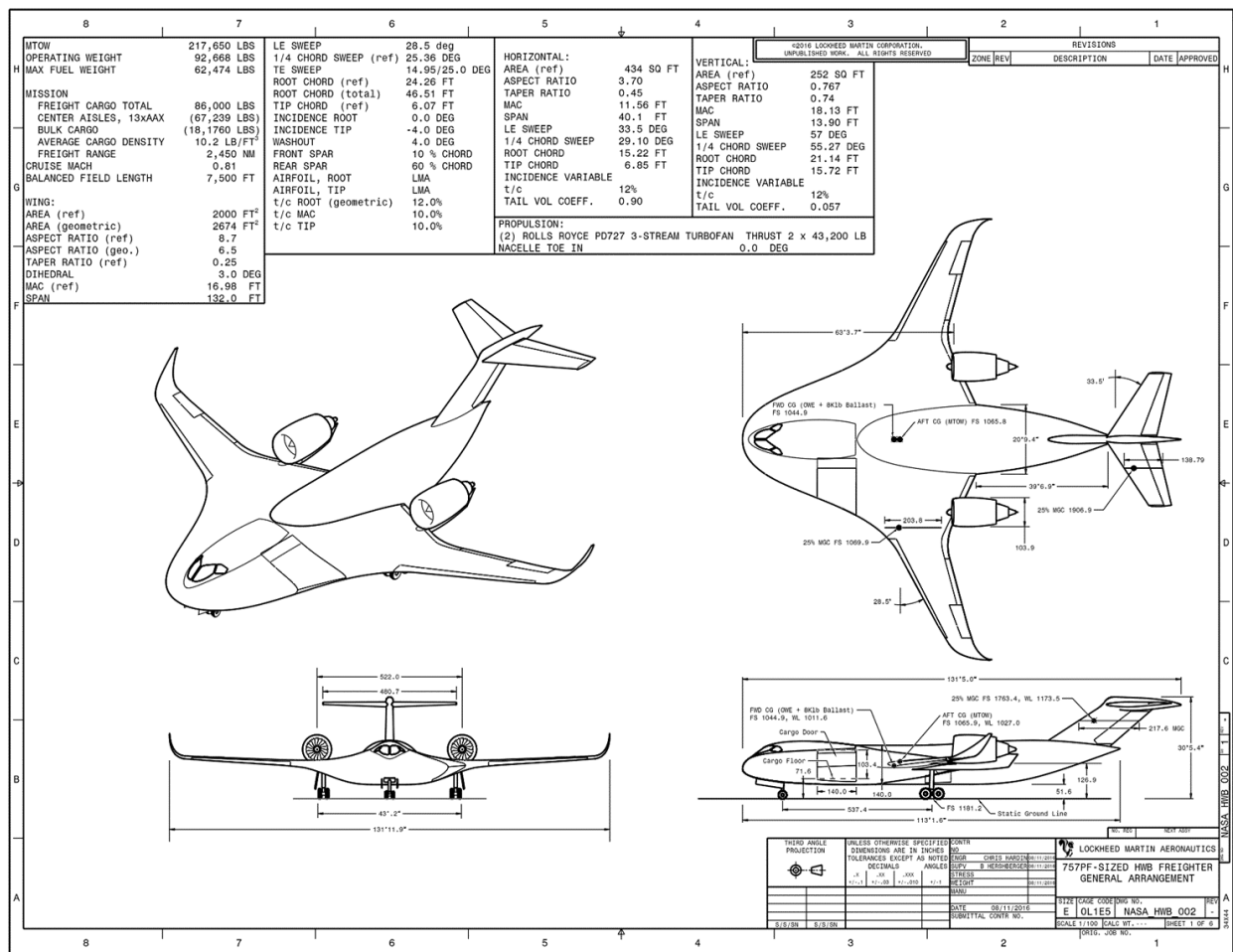
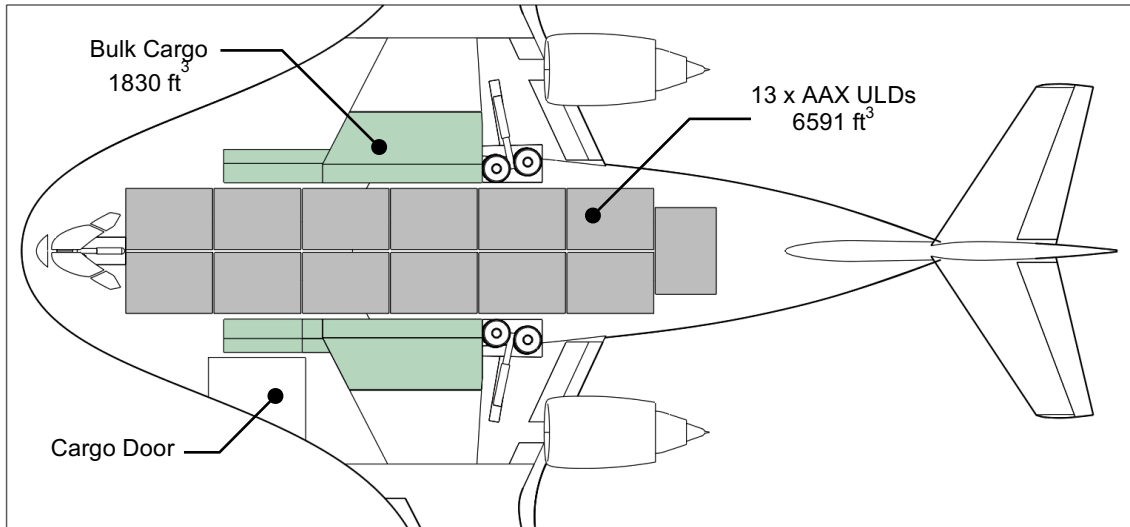


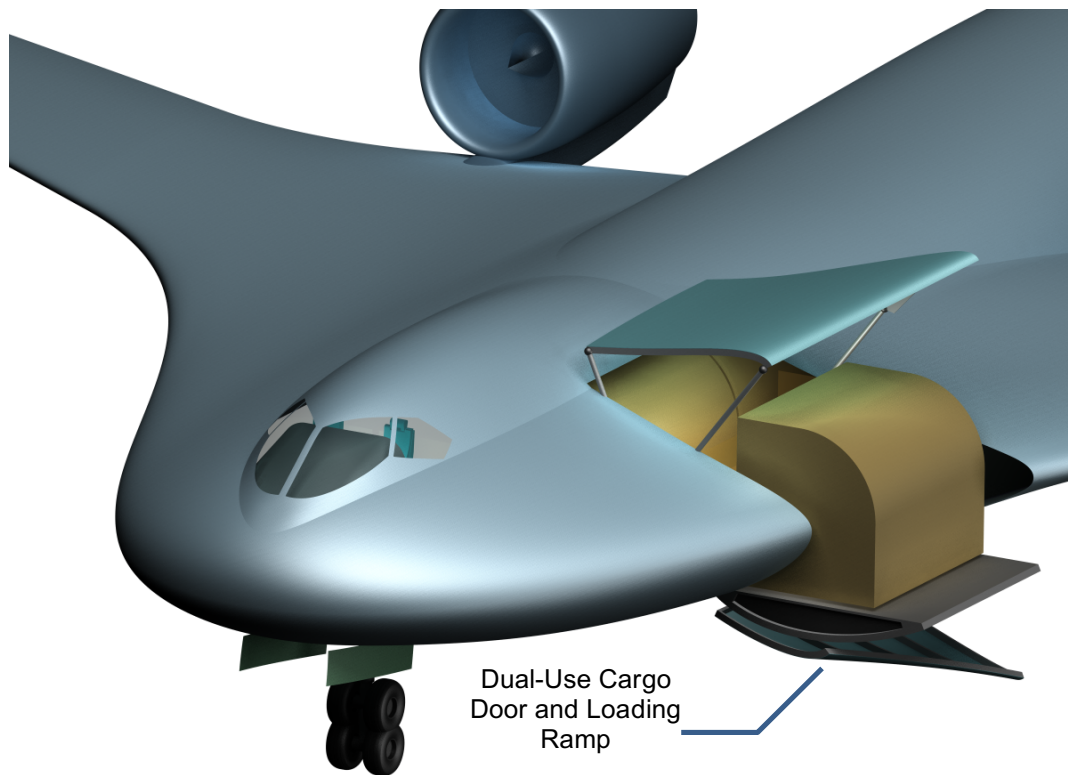
Figure 14: General Arrangement Drawing for the HWB B757F Sized Freighter.





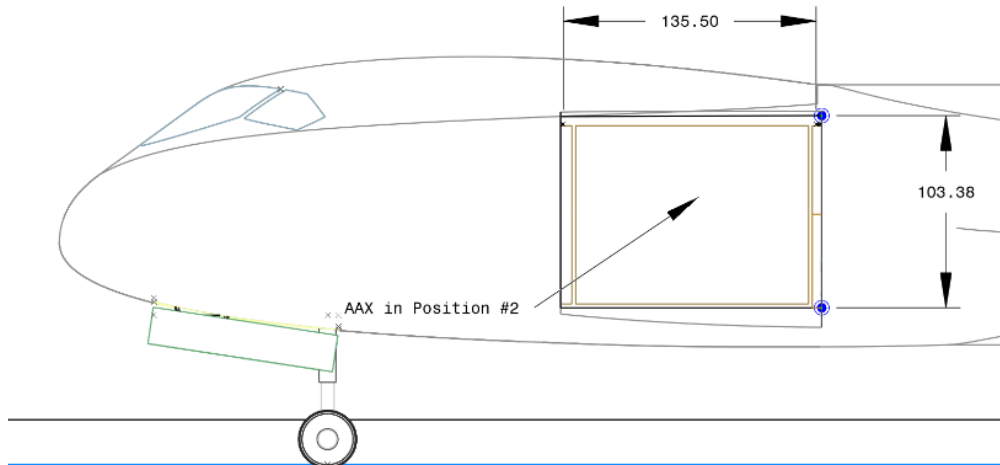
**Figure 15: HWB 757 Cargo Bay Configuration.**

For loading, a main cargo door was placed on the left side of the aircraft ahead of the wing, as is the case with the 757PF (Figure 16 and Figure 17). The 757PF main deck door dimensions are W 134” x H 86”. For the HWB, they are 135.5” x 103.4”. Extra height was needed to accommodate the AAX container type, which is 96” tall. The cargo door was added after discussions with United Parcel Service (UPS), which indicated current operations require a side cargo door.



**Figure 16: Side Door Loading of AAX Container.**



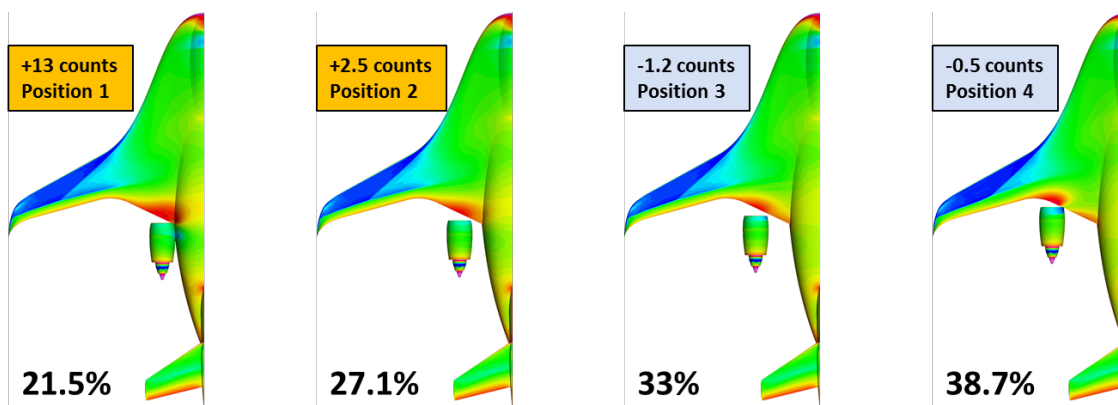
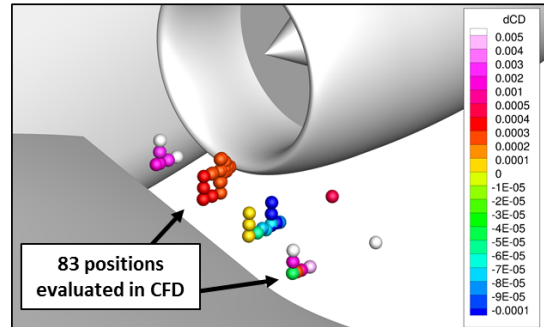


**Figure 17: 757PF-Sized HWB Freighter Cargo Door.**

AAX containers are first loaded through the cargo door and then pushed into the aft-most cargo positions. For this procedure, points in the CG excursion envelope were used to verify that the center of gravity would remain ahead of the main gear contact point.

The aerodynamic assessment and optimization effort is described in detail in the “Advanced HWB Based 757F Replacement Design Report.” Key results from that assessment follow. Results from an engine placement study are depicted in Figure 18.

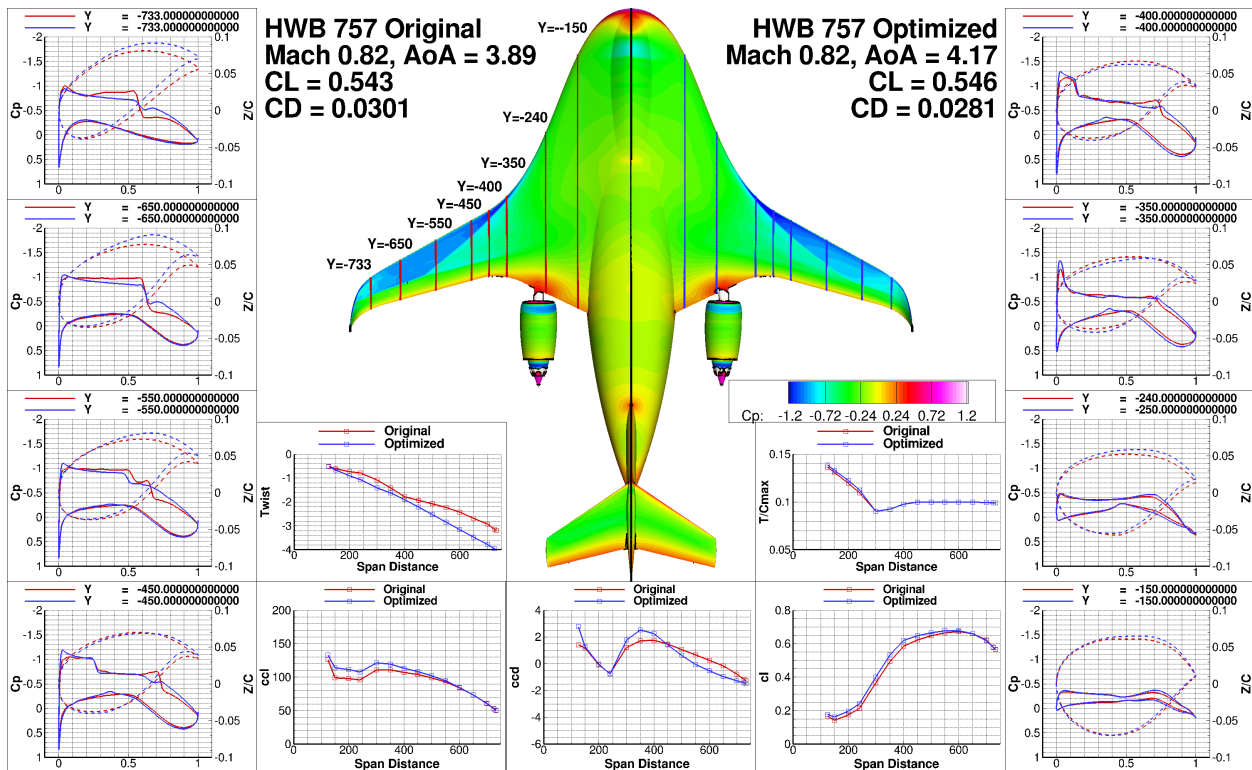
- **4 Different span locations chosen (no pylon)**
- **X and Z position of engine were optimized to determine best location at each span**
- **Results plotted where each point represents the lower leading edge of the engine**
  - $dCD = \text{Integrated } CD - \text{Clean } CD - \text{Isolated Engine } CD$
- **-1.2 drag count favorable interference at 33% span location, Mach 0.83**



**Figure 18: Results from HWB 757 Engine Placement Study.**

From this figure it can be seen that 83 different engine positions were evaluated in CFD. Results indicated that the optimum engine position resulted in 1.2 counts of favorable interference drag compared to the isolated aircraft and isolated engine performance.

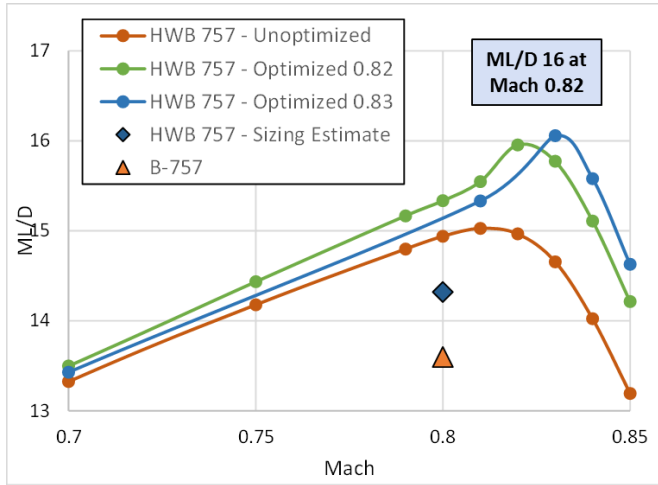
After the baseline CFD simulations were completed, KNOPTER was used to optimize the configuration for improved performance. A comparison of the baseline and optimized surface pressure distributions, airfoil shapes, wing span load, and wing twist is depicted in Figure 19. From this figure it can be seen that the optimization significantly reduced the wing shock strength along the wing span and resulted in a 20 count drag reduction at cruise conditions (Mach=0.82, CL=0.54).



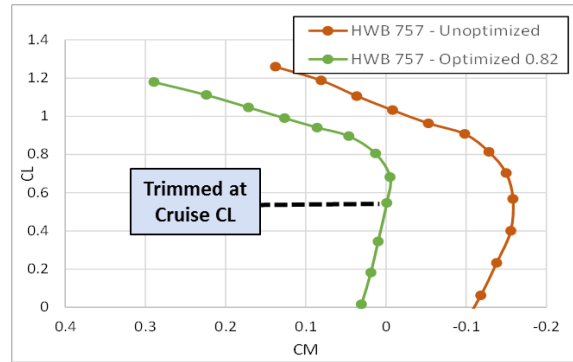
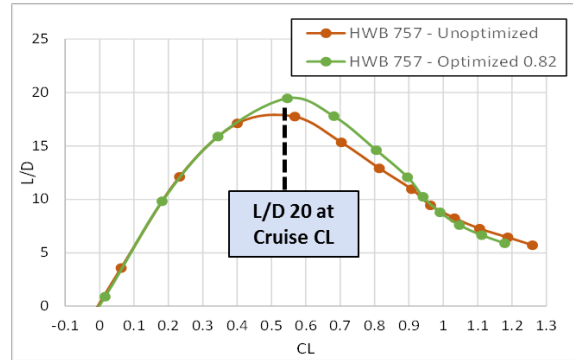
**Figure 19: KNOPTER Based Optimization Results on the HWB 757 Freighter Configuration.**

The drag rise for both the baseline and optimized configurations is depicted in Figure 20 with aerodynamic efficiency (as measured with Mach \* Lift / Drag) plotted as a function of Mach number. This figure depicts the large improvement in performance (6.7%) associated with the KNOPTER optimization process, highlighting a peak ML/D of 16 is achieved at a cruise Mach of 0.82 (as indicated with peak aerodynamic efficiency). Also depicted in this figure is the estimated performance from the sizing effort with the lower fidelity aerodynamic estimation methods (shown with the blue diamond). This highlights that the conceptual design tools typically underestimate the aerodynamic efficiency of the HWB configuration by approximately 11%. This is in contrast to the conventional tube-and-wing configuration results from Figure 7 that showed the initial sizing estimate results to be very close to the final optimized performance for the conventional tube-and-wing configuration.

- Optimizations performance at Mach 0.82 and 0.83
- Mach 0.83 achieved better ML/D but penalized off-design Mach's
- Mach 0.82 optimization resulted in trimmed solution with 6.7% improved aero efficiency
- 17.6% better aero than B-757



CL 0.543, 39k ft



Mach 0.82, 39k ft

Figure 20: Pre-and Post Optimization HWB 757 Aerodynamic Performance Comparisons.

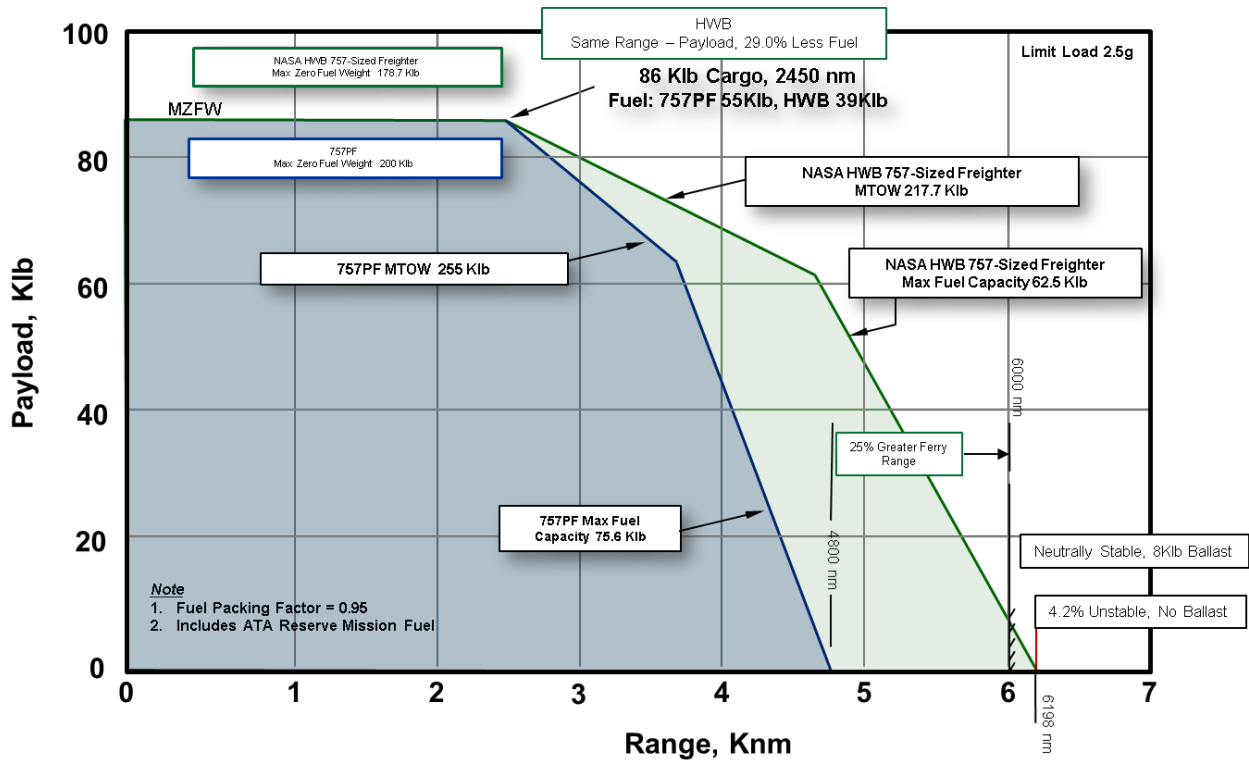


Figure 21: NASA HWB 757 Freighter Payload-Range.

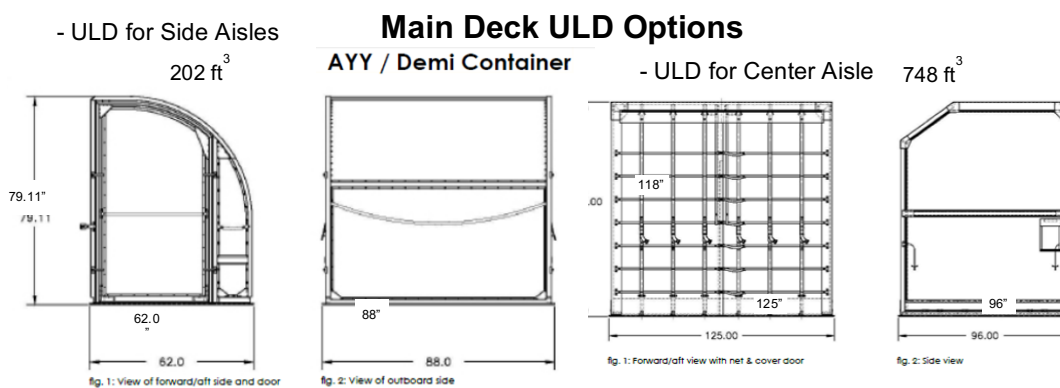
A payload-range diagram was created using the mission performance model and is compared with the baseline 757F as shown in Figure 21. Results indicated a 29.0% reduction in fuel usage at the same range / payload design point. Larger fuel usage reductions result for longer range missions. Results also indicated the potential for a 25% increase in aircraft ferry range.

### B777 Sized HWB Freighter

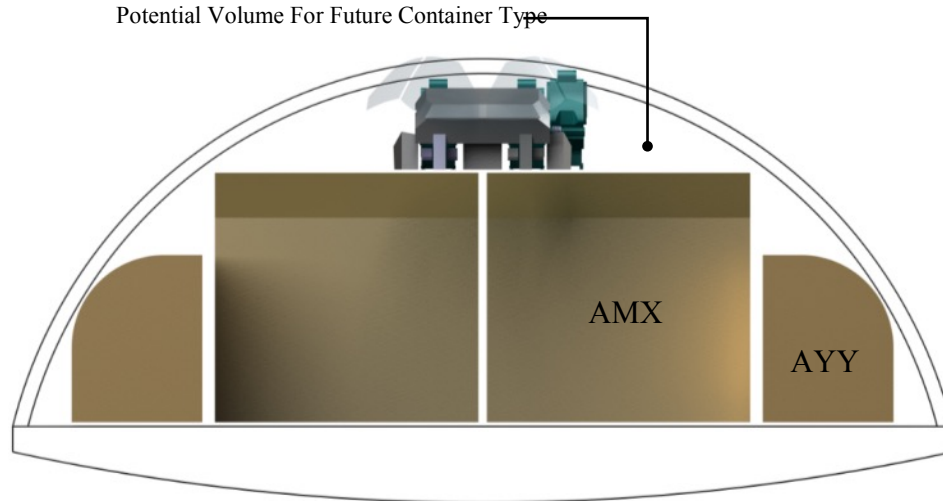
The objective of this task is the development of a conceptual aircraft design capable of performing the Boeing 777-200LR derived freighter (777F) mission using an HWB vehicle configuration and to understand the impact modern technology (advance aerodynamic design tools, high bypass ratio engines, and advanced lightweight materials) has on mission performance. Technology levels applied are assumed to be available for an EIS date of 2035-2040. The resulting configuration is described in detail in the “Advanced HWB Based 777F Replacement Design Report” delivered as part of this effort. The following provides an overview of the 777F sized HWB freighter development.

In order to predict vehicle performance, a loft of the vehicle OML was required to provide basic dimensions (wetted areas, lengths, volumes, etc.). Before starting the loft, a cargo bay definition, sized to the payload and volume requirements, was needed. Here, a trade study was performed to determine the best cargo bay configuration for the HWB 777 shape. A survey of cargo container types was made to find shapes that best suited the HWB cross section characteristics.

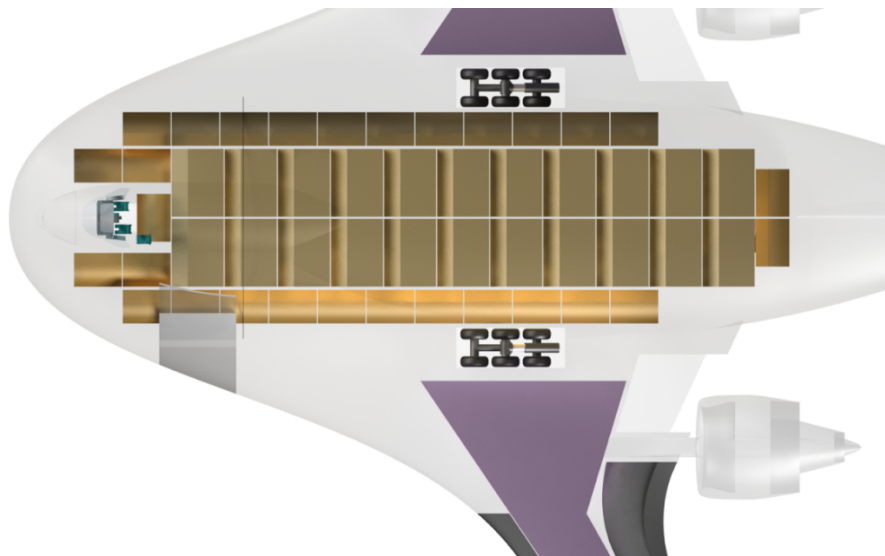
Two container types shown in Figure 22 were down selected from the 13 main deck ULD types available in (Satco Inc., 2010). A smaller container type, the AYY, was selected for use in the HWB side aisles. The AYY Demi is used by A300, A310, B727, B757PF, DC-10 and MD-11. The larger container, the AMD, selected for the center aisles is used primarily by B747F and B747Combi freighters. Figure 23 shows a section view of the cargo bay with ULDs loaded. A planform view of the final cargo bay is shown in Figure 24.



**Figure 22: Two ULD Types Selected for HWB 777 Cargo Bay.**



**Figure 23: Cargo Bay Section View with AMX and AYY ULDs.**



**Figure 24: Planform View of Final Cargo Bay Configuration Layout (29 AYY + 22 AMX).**

With the cargo bay dimensions determined, a surface loft of the vehicle OML was created in CATIA (Figure 25). The loft is parametric and provides basic dimensional data used to predict cruise aerodynamic performance and component weights for analysis. Principal parameters (independent variables) are: wing area, aspect ratio, wing leading-edge sweep, wing taper ratio, wing average thickness, wing longitudinal position and engine scale factor. Tails were sized using historical volume coefficients, 0.057 for the vertical and 0.90 for the horizontal. Also, as changes are made to wing area, sweep or wing longitudinal position, tail areas automatically adjust to keep tail volumes constant.

As described in detail in the “Advanced HWB Based 777F Replacement Design Report,” a sizing study was performed to determine the optimum vehicle size. The OML surface loft was then updated to reflect the new characteristics. A general arrangement drawing of the optimized HWB 777 freighter is depicted in Figure 26.

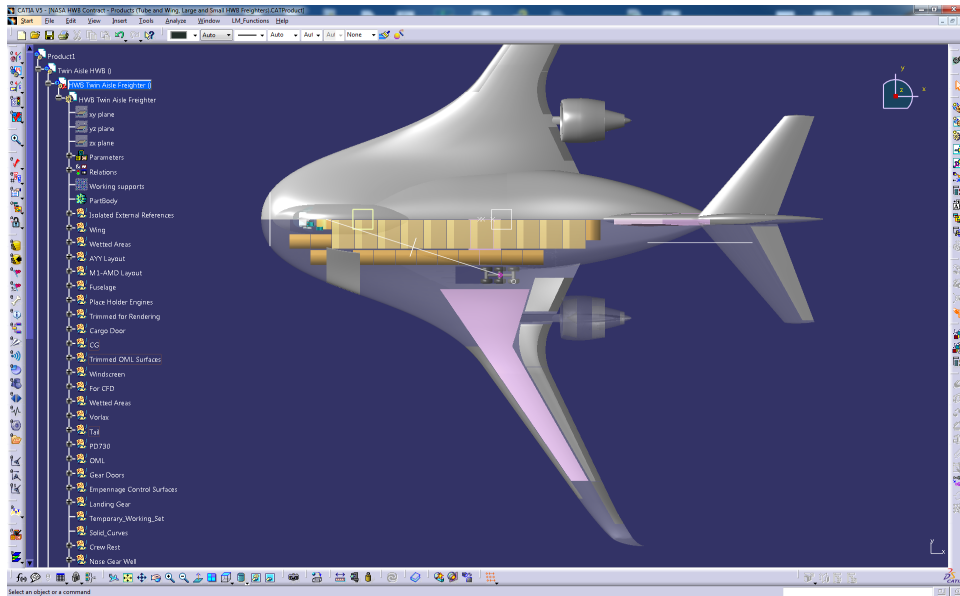


Figure 25: Parametric CATIA Model for the 777F Sized HWB Freighter.

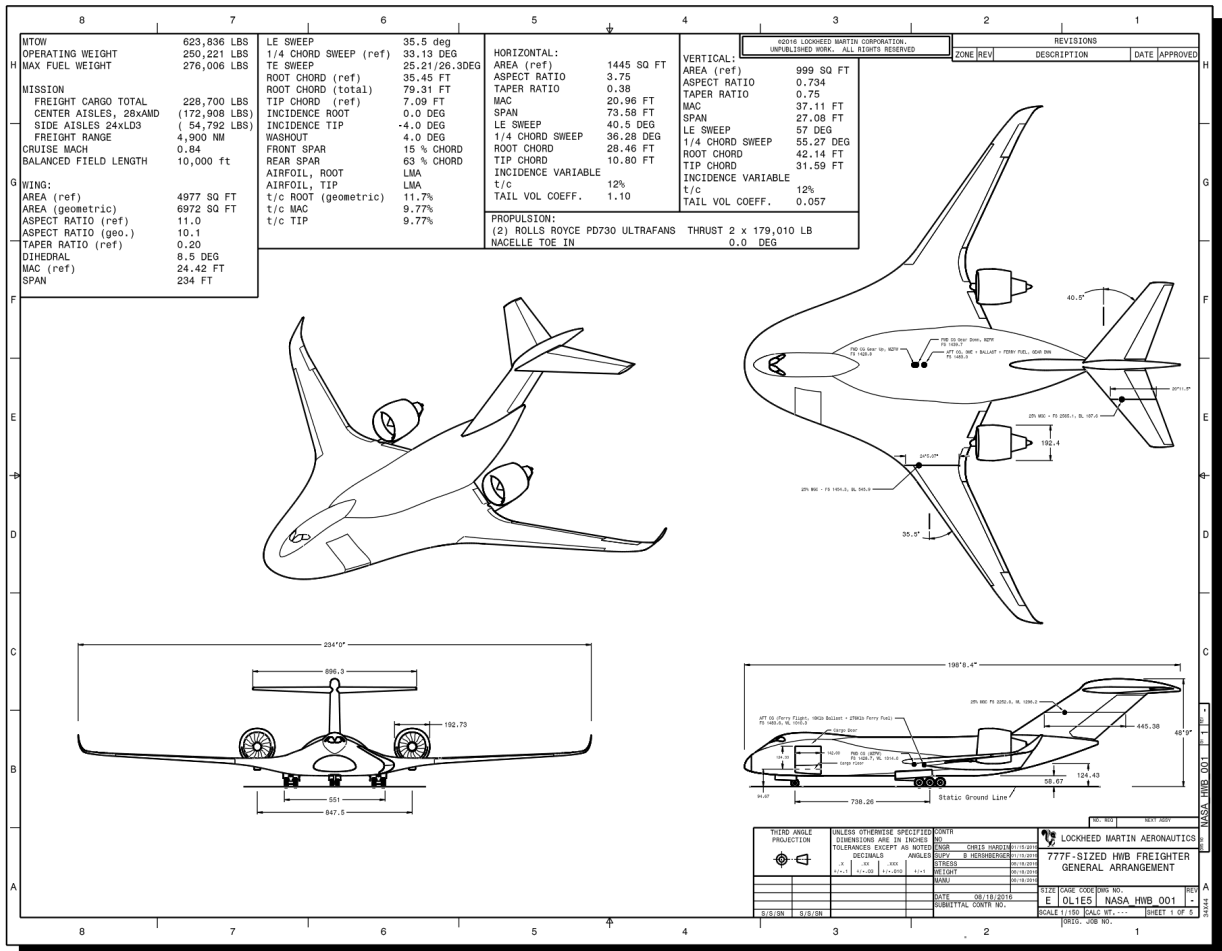
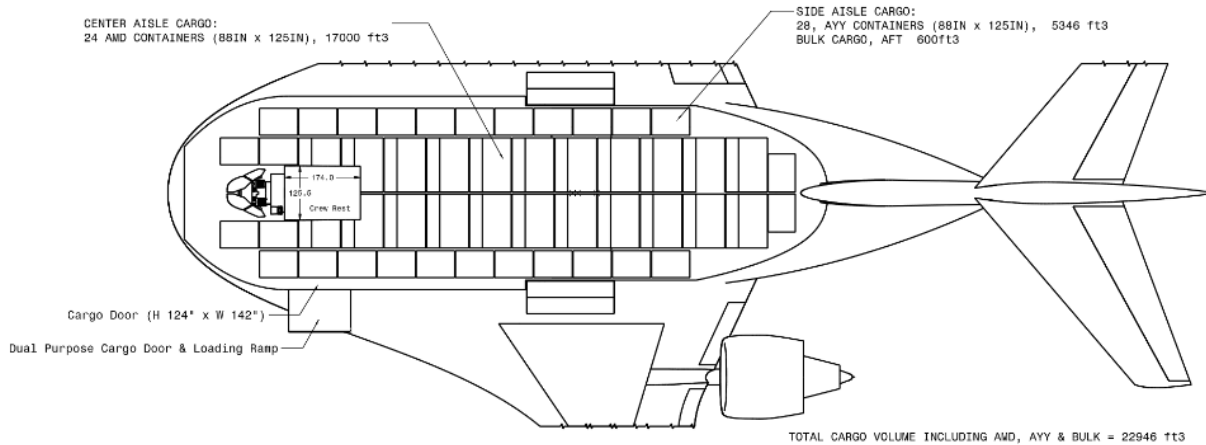


Figure 26: General Arrangement Drawing for the HWB 777 Sized Freighter.

Figure 27 shows the internal arrangement configured with 24 AMD unit load devices on the main cargo deck. 1320" (110') of deck length was required assuming a 2" spacing (fore-aft) between ULDs loaded 2 abreast with 4" spacing (left-right) on centerline. The cargo door was positioned at the front of the aircraft. An aft cargo door position was considered but excluded due to the proximity of the engines and inability of the loader to properly approach the vehicle in that area. The cargo door was placed on the left side of the aircraft, as is the case with the 777F. Cargo door dimensions match or exceed that of the 777F (W 142" x H 120"). The door opening in this design is W 142 x H 124". Some margin in height was added to account for ULD loading system rollers that sit on the main deck floor.

Loading the aircraft from the front presents the potential for the aircraft to tip back on its tail. This scenario was analyzed. It was found that with all ULD positions populated aft of the main gear attachment point FS 1514, the aircraft CG was 26" forward of the main gear aft contact point, FS 1571. Tipback will not occur provided the main gear truck can be locked to prevent rotation about its trunnion since the CG is aft of the trunnion point.



**Figure 27: HWB 777 Cargo Floor Arrangement.**

Results from the KNOPTER based optimization of the HWB 777 configuration are depicted in Figure 28. This figure highlights the baseline lofted and KNOPTER optimized surface pressure distributions, airfoil shapes, wing span load, and wing twist distributions. Of particular note from this figure is the large increase in inboard sectional wing loading ( $c^*c_l$ ) and corresponding reduction in outer wing loading. The figure also highlights the large reduction in outer wing shock strength that was achieved with the combination of the optimization and increased inboard wing thickness.

The final aerodynamic performance of the optimized HWB 777 configuration is depicted in Figure 29. This figure highlights that the optimization significantly increased the cruise Mach number and overall trimmed aerodynamic efficiency of the configuration. In addition, it highlights that the addition of trim tanks (described in detail in the "Advanced HWB Based 777F Replacement Design Report") eliminated trim drag at the design cruise point ( $CL=0.55$ ).



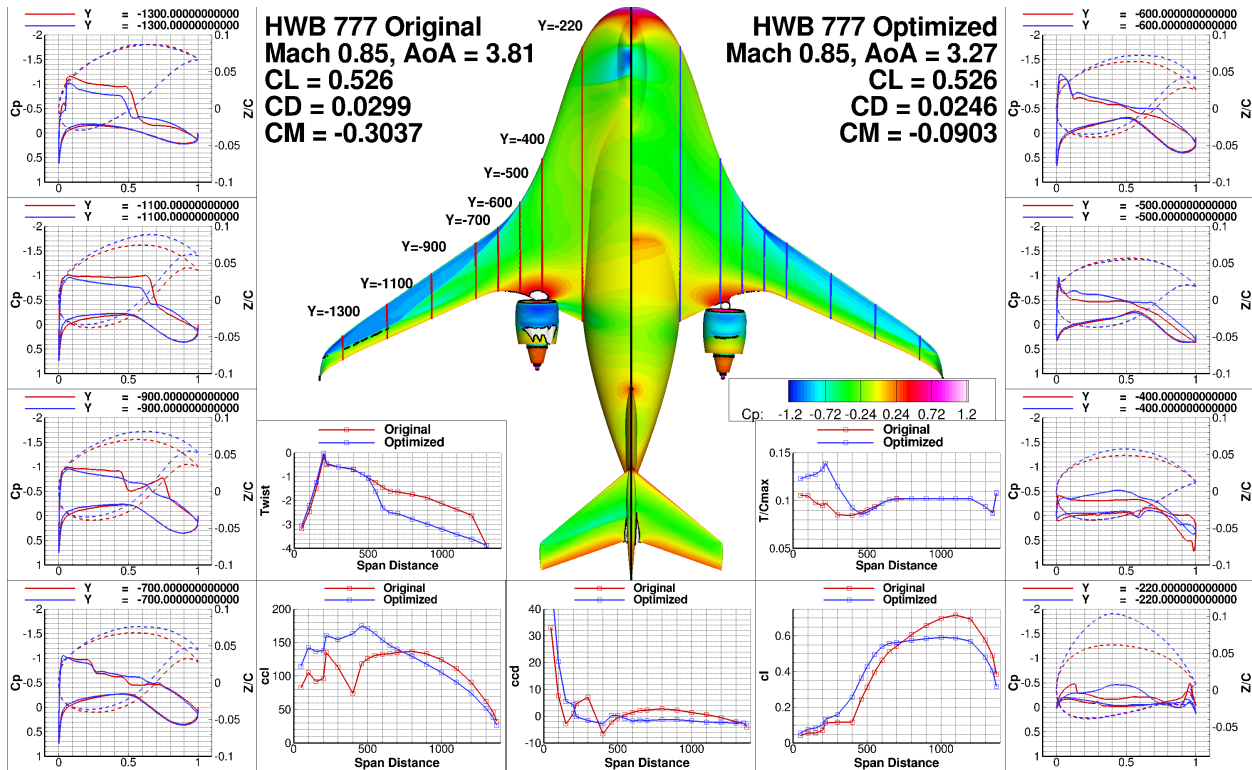


Figure 28: HWB 777 Aerodynamic Optimization Results.

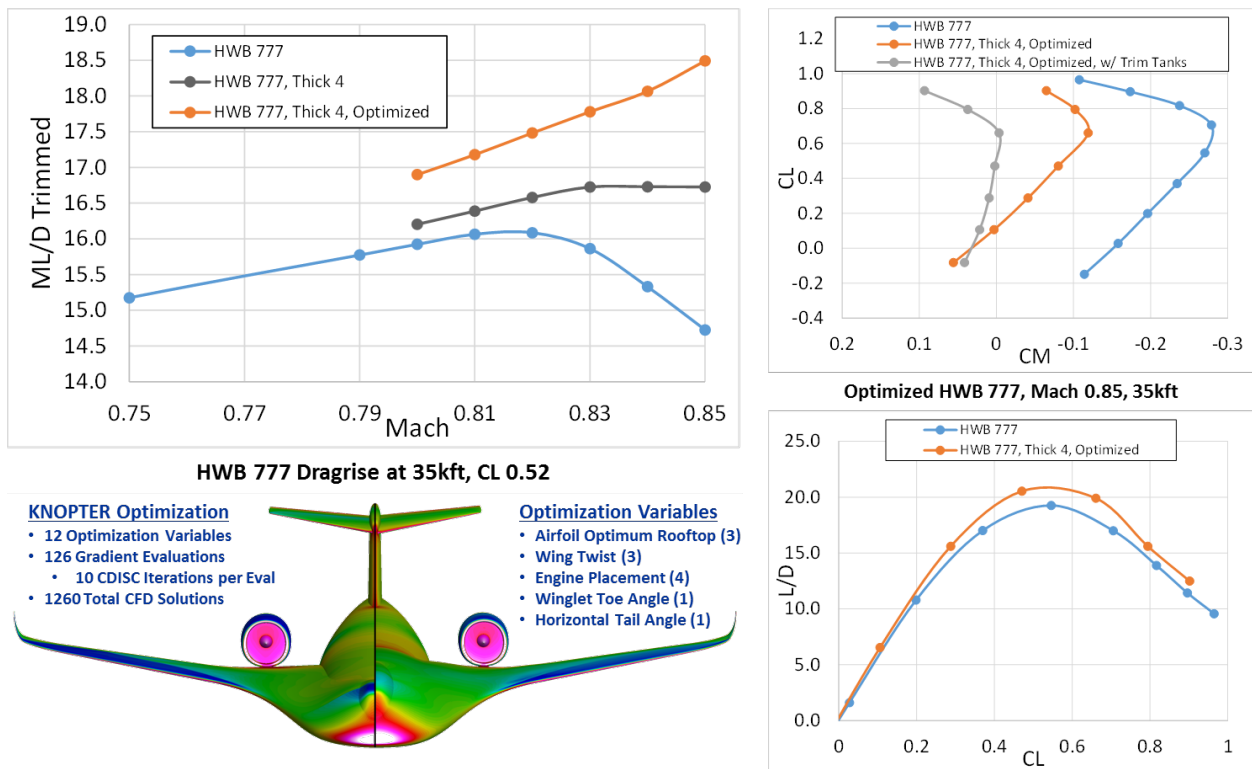


Figure 29: HWB 777 Final Aerodynamic Performance.



A payload-range diagram (Figure 30) was created using the mission performance model and is compared with the 777F. The U.S.-Asia sector is the fastest growing air freight sector in general. The two busiest freighter airports in this segment is the Hong Kong to Memphis route. The range for that mission (~7000 nm) and the maximum payload each platform could carry for that range was used to calculate overall fuel savings. Results indicated for this route a 51% fuel savings.

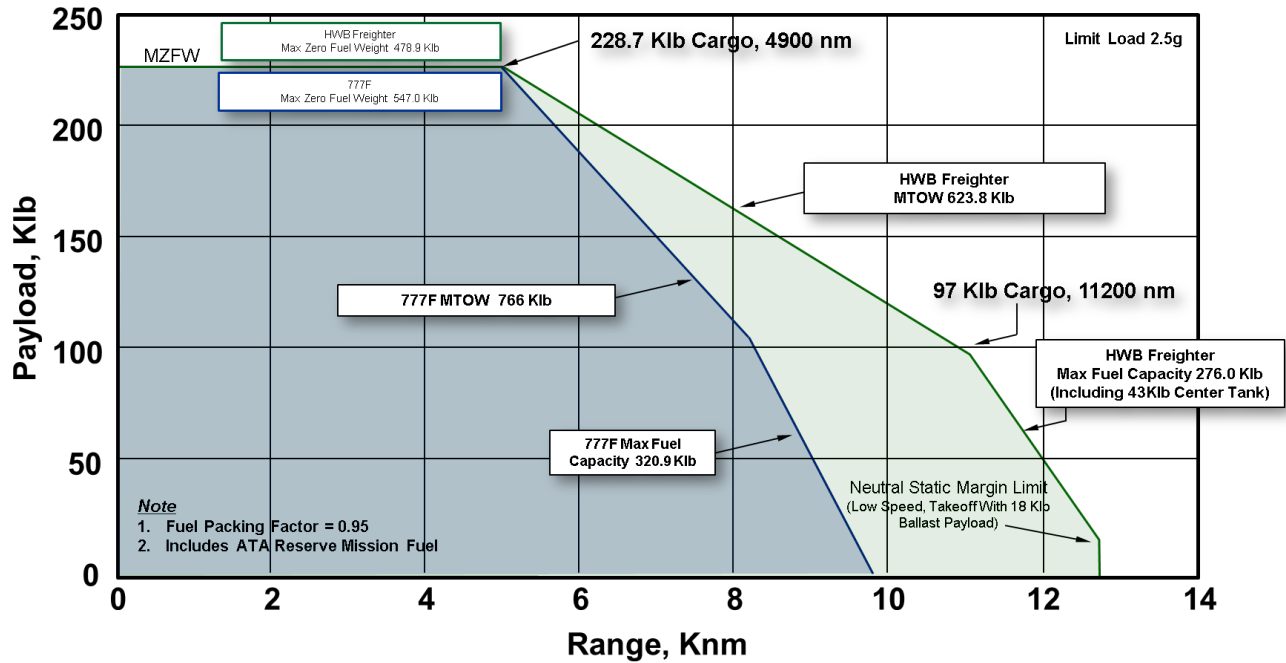
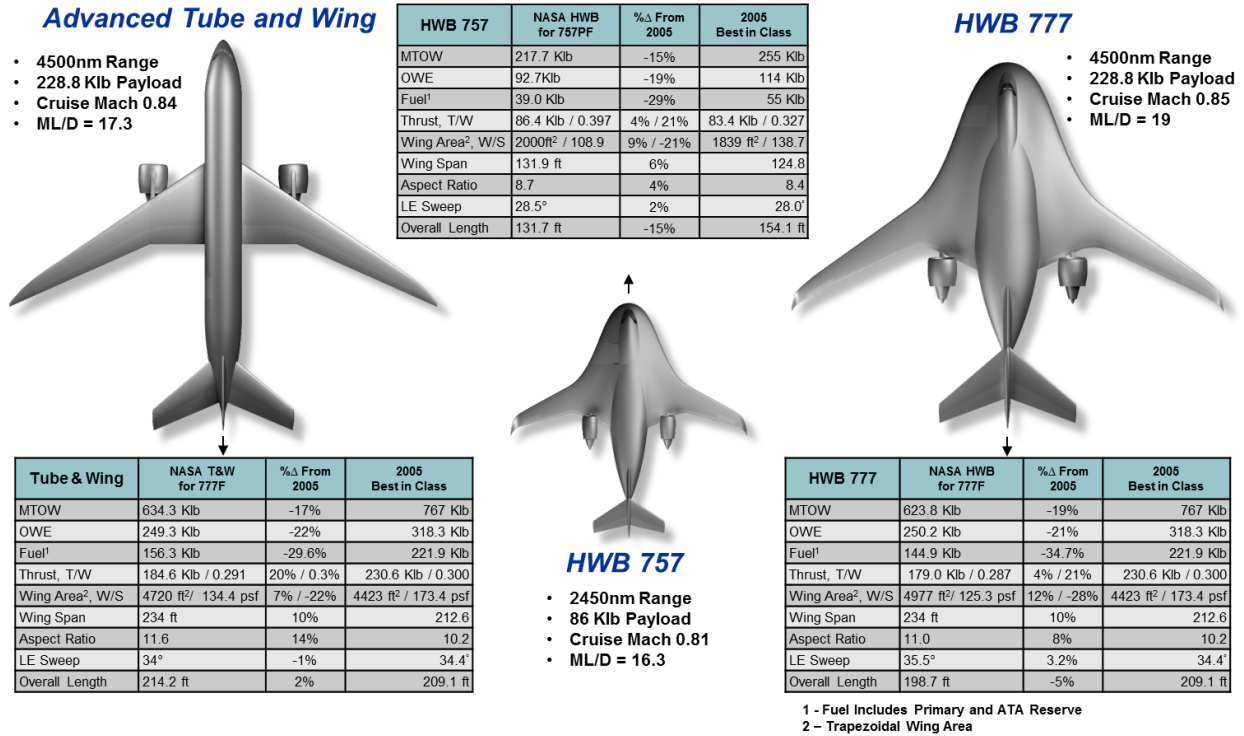


Figure 30: NASA HWB 777 Freighter Payload-Range.

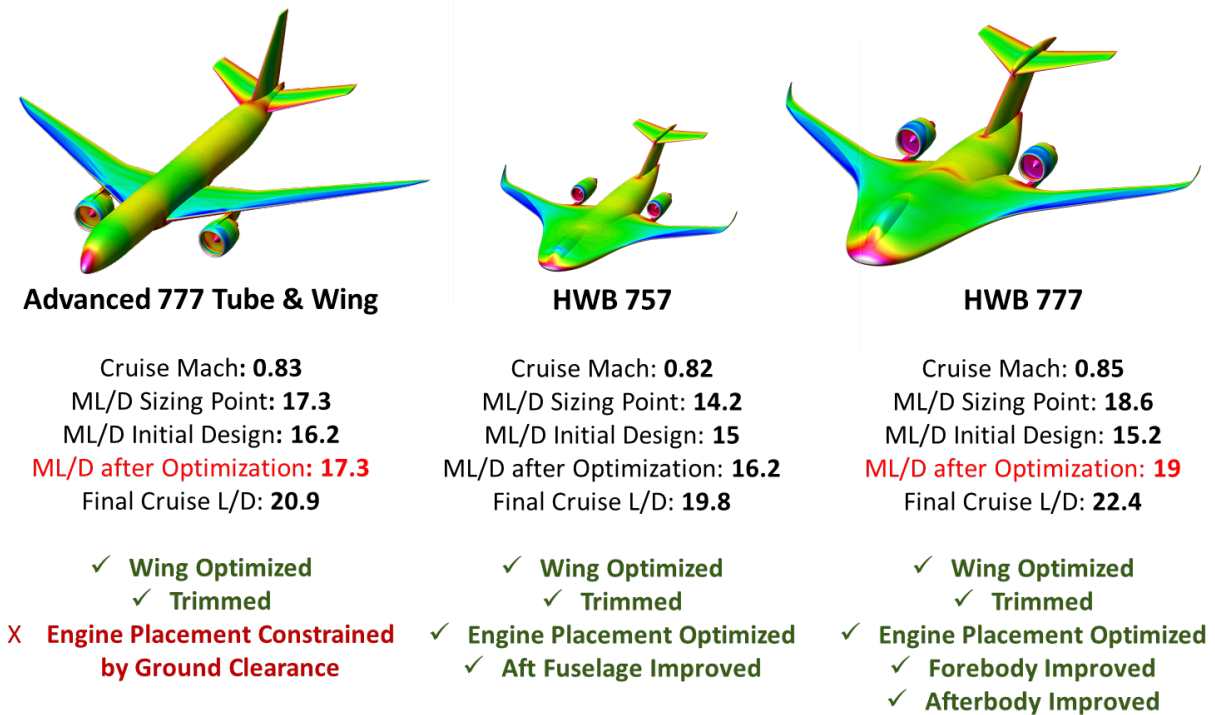
### Summary of Results from Configuration Design Studies

This section summarizes the key findings / lessons learned from the configuration design studies. The overall performance characteristics of each of the three configurations developed as part of this effort are depicted in Figure 31 along with a summary of the design mission. This figure highlights that the operating weight empty (OWE) of the 777F sized advanced tube-and-wing and HWB configurations are nearly identical. It also highlights that the HWB uses 7.3% less fuel for the design mission than the advanced tube-and-wing configuration. This fuel savings increases as range is increased past the 4,500nm design range at maximum payload.

A summary of the aerodynamic performance characteristics of the three configurations is depicted in Figure 32. From this figure it can be seen that the aerodynamic performance of the 777F sized HWB is 10% higher than a comparable advanced tube-and-wing configuration of similar technology levels (as measured with Mach \* Lift / Drag). It also highlights that the much smaller 757 sized freighter also has excellent aerodynamic efficiency, which equates to an estimated 60% reduction in fuel usage compared to today's B757 freighters.

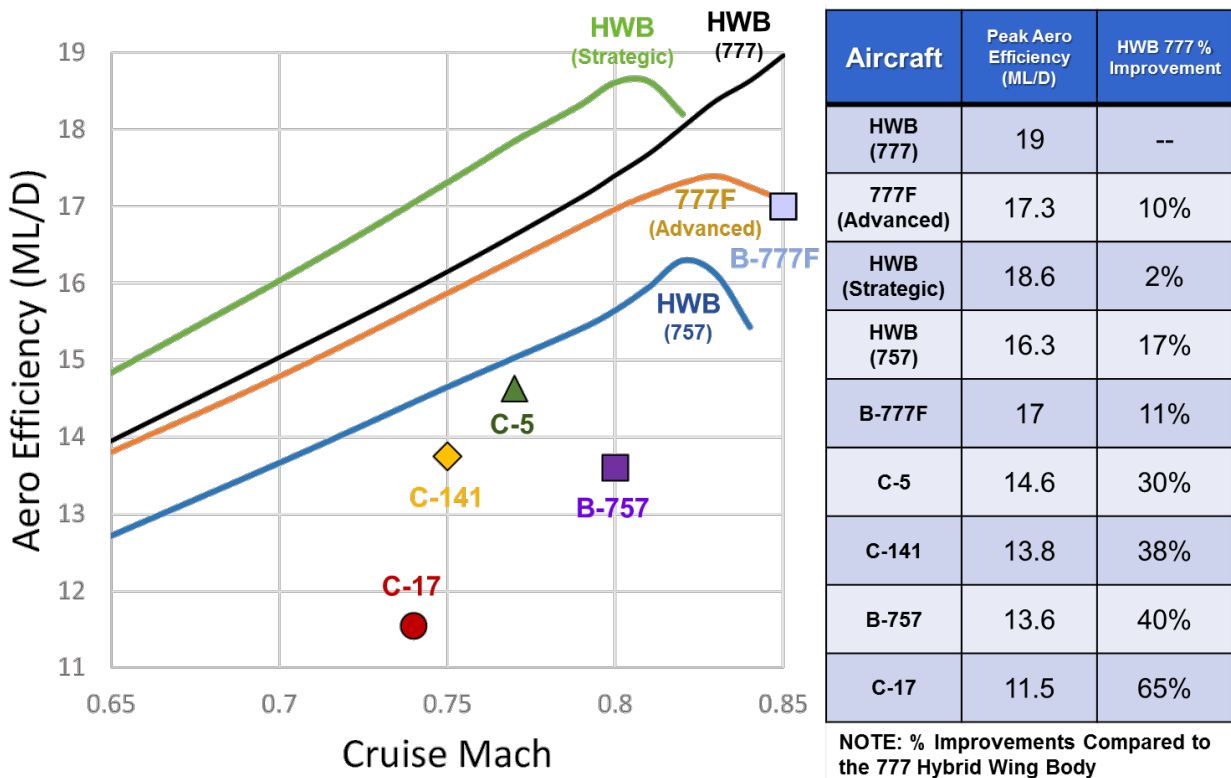


**Figure 31: Summary of Key Performance Characteristics of the Three Configurations Developed as Part of this Study.**



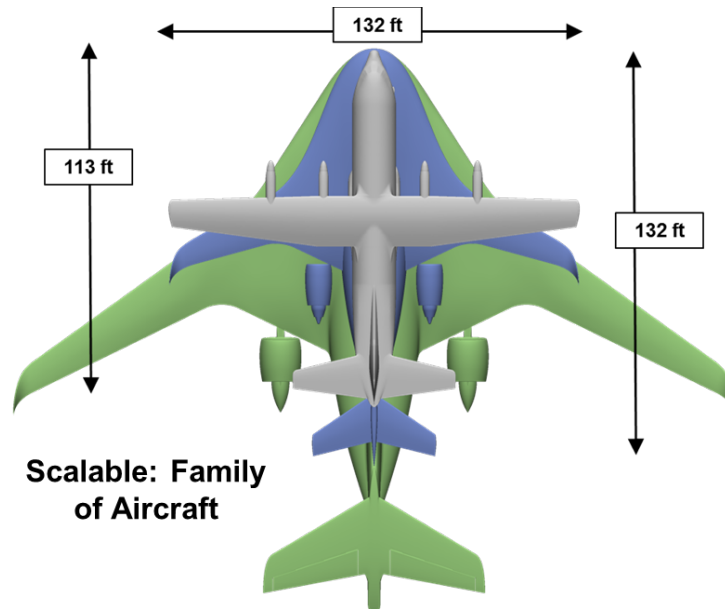
**Figure 32: Summary of Aerodynamic Performance Characteristics of the Three Configurations Developed as Part of this Study.**

A comparison of the aerodynamic efficiency of the three configurations developed as part of this effort (i.e., HWB 777, 777F Advanced Tube-and-Wing, and HWB 757) along with other existing aircraft is depicted in Figure 33. Also depicted in this figure is the aerodynamic performance of the original HWB military airlifter (HWB Strategic) developed under the AFRL sponsored RCEE program. This figure highlights the large increase in aerodynamic efficiency possible with the hybrid wing body configuration. It also highlights a key finding from this study -- that the performance of the HWB is scalable from a relatively small 757 sized freighter to a large 777 sized freighter. This is a critical finding that answers one of the primary questions going into the study. Another important finding was that the HWB 777 achieved a cruise speed of  $M=0.85$  or higher. This is significantly higher than the  $M=0.81$  cruise speed achieved with the HWB strategic military airlifter. As described in a following section, this was enabled with increased inboard wing thickness.



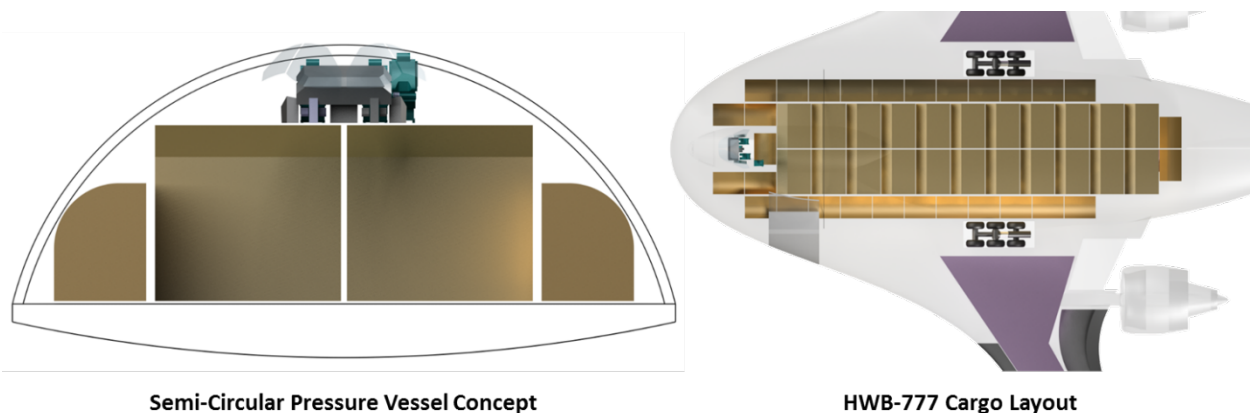
**Figure 33: Aerodynamic Performance Comparisons between Configurations Developed for this Study and Existing Aircraft.**

The scalability of the HWB configuration is illustrated in Figure 34, which depicts the 777 sized HWB configuration (green), the 757 sized HWB (blue), and an existing C-130 (gray). This figure highlights that the overall HWB concept is easily scalable to a family of aircraft.



**Figure 34: HWB Scalability Comparison.**

Another key finding from the study involved a new semicircular fuselage cross sectional shape for HWB configuration. As depicted in Figure 35, inside the fuselage OML, cargo is carried in a pressurized volume having a semicircular cross section. Providing that the cross section frames are attached to a sufficiently rigid structure (cargo floor), they will retain their shape when pressurized without requiring vertical tension ties. The cargo floor (approximately 3' deep at centerline) forms the lower pressure boundary. The upper boundary is located outside of 7" deep semicircular frames. The arrangement is similar to that found in conventional fuselage construction. The OML and its backing structure are fastened to the semicircular frames. Local pressure and skin friction loads are carried through the backing structure that transmits them to the primary structure. This fuselage cross sectional shape is a potentially lighter option than the structural concepts previously studied, which are similar to the HWB 757 layout depicted previously.

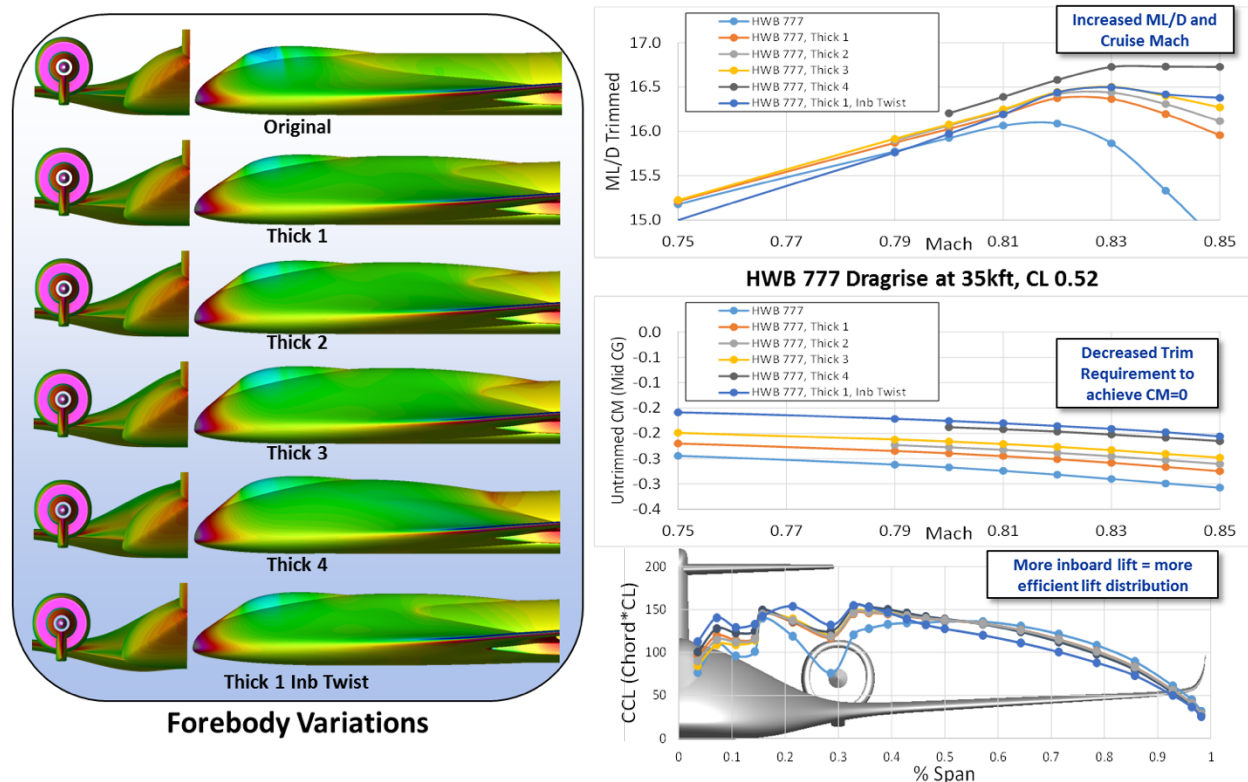


**Semi-Circular Pressure Vessel Concept**

**HWB-777 Cargo Layout**

**Figure 35: Semicircular Fuselage Cross Sectional Shape for the HWB.**

Another important finding was the sensitivity of aircraft performance to inboard wing thickness. As depicted in Figure 36, numerous variations in inboard wing thickness were evaluated and the impact on aerodynamic performance was evaluated. From this figure, it can be seen that increasing inboard wing thickness increased overall aerodynamic efficiency (as measured with Mach \* Lift / Drag) and the cruise Mach number, while also reducing overall trim drag. As also depicted in this figure, the increased inboard wing thickness significantly increased inboard wing loading and effectively reduced outer wing loading. This result was also highlighted in Figure 28, which depicted the large increase in inboard sectional wing loading ( $c \cdot c_l$ ) and corresponding reduction in outer wing loading. The figure also highlighted the large reduction in outer wing shock strength that was achieved with the combination of the optimization and increased inboard wing thickness. This effect resulted in the increase in the achieved cruise Mach number as the drag divergence Mach number was primarily driven by the outer wing shock strength, which is a direct function of outer wing load.



**Figure 36: Increased Inboard Wing Thickness Study Results.**

Results from aft fuselage shaping studies are depicted in Figure 37. Results from this study indicated that the mobility compatible upswept aft fuselage generated 4.6 counts more drag than the optimized commercial freighter compatible aft fuselage (nonupswept afterbody with rounded corners). Surprisingly, results also indicated that a streamlined cylindrical aft fuselage (cylindrical afterbody) actually had 0.5 counts more drag than the much wider optimized fuselage shape. Results from yehudi studies are depicted in Figure 38. This figure highlights that the yehudi can be moved inboard to butt line 415" without impacting overall aerodynamic performance. The advantage of this position is that it permits additional inlet noise shielding and allows the engine to move forward, helping with aircraft center of gravity.



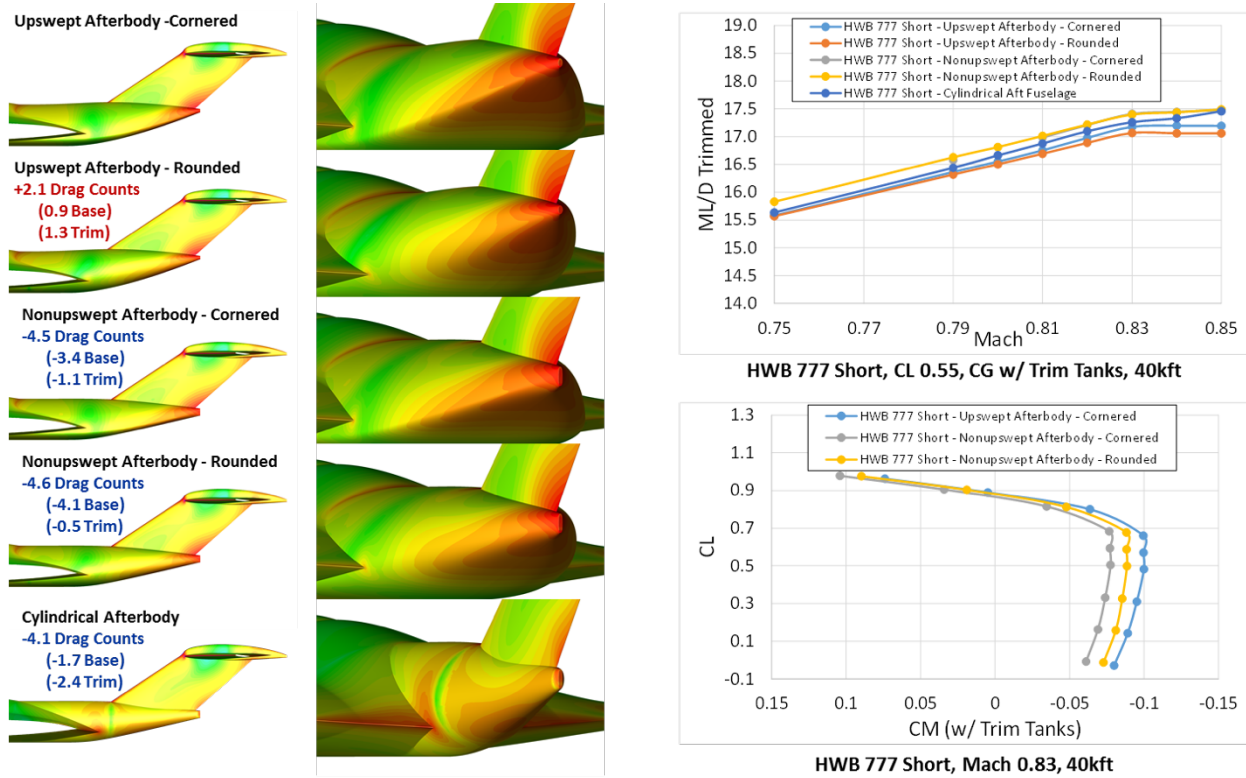


Figure 37: Aft Fuselage Study Results.

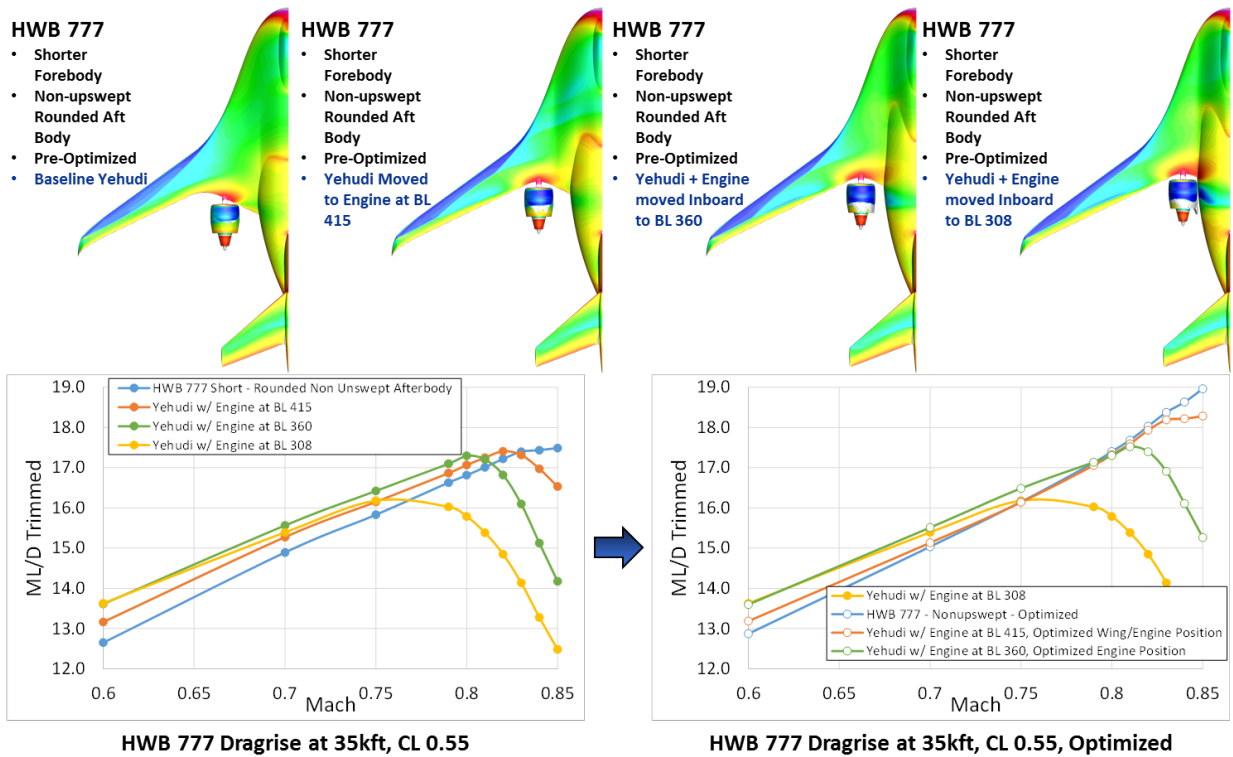
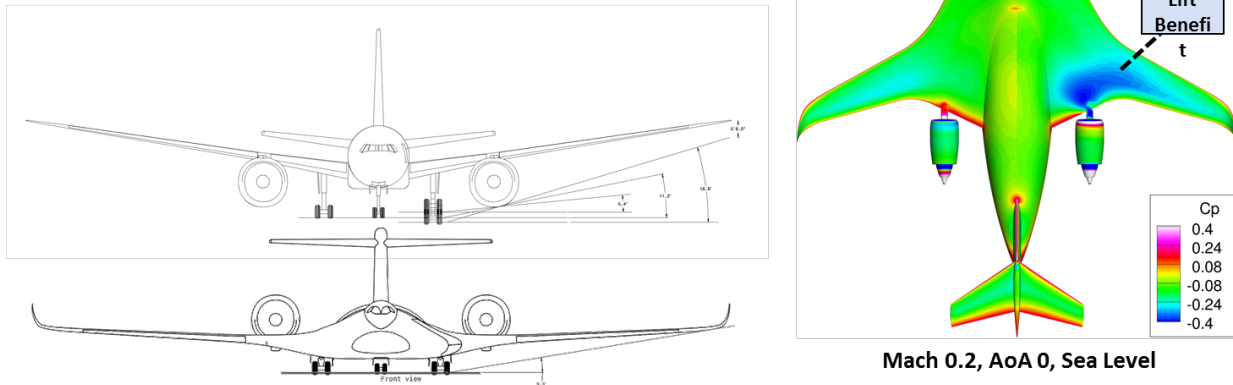


Figure 38: Yehudi Study Results.

One final result of note is the benefit associated with the over-wing nacelle (OWN) engine placement. As summarized in Figure 39, in addition to the transonic cruise efficiency benefit confirmed with the National Transonic Facility (NTF) wind tunnel testing (Reference 8), the OWN technology also leads to significantly shorter landing gear. This results in an overall reduction in landing gear weight as well as helping to reduce landing gear noise, which is the primary noise generator for the aircraft. Also highlighted in this figure is the low speed powered lift benefit that results from the OWN engine integration. This benefit results from the increased suction on the wing upper surface due to the acceleration of the flow into the inlet at low speed conditions.

### Over-Wing Mounted Nacelle Benefits

- Demonstrated aero integration benefit
- Demonstrated powered lift benefit
- Shielded inlet reduces susceptibility to FOD
- Acoustic shielding of forebody reduces noise
- Reduced landing gear length compared to under-wing mounted nacelle
- Allowable bank angle increased for cross wind landing
- Jet engine exhaust velocity contours reduced for ground operation
- Jet exhaust height reduces ground service operating temperatures



**Figure 39: Over-Wing Nacelle Benefits.**

### Market Study Results Summary

This section summarizes the results from the market study documented in detail in the “AHWB Commercial Cargo Market Study and Cost Analysis Report.” A detailed market study was performed to establish the need for HWB aircraft and its associated technology. As depicted in Figure 40, this assessment included both military and commercial opportunities as the dual use potential of the aircraft significantly expands the market size. The market study was based upon extensive market research, as well as results from meetings with the UPS Director of Procurement. From this figure it can be seen that there is a need for as many as 1,815 HWB based airliners, tankers, and commercial freighters over the next 20 years. As documented in Figure 41, results from our market research (documented in detail in the “AHWB Commercial Cargo Market Study and Cost Analysis Report”) confirmed the need for a new 777 sized commercial freighter in the

2025 timeframe. This figure highlights the concern of commercial freighter companies (such as UPS) in the availability of this class of new aircraft in the 2025 timeframe.

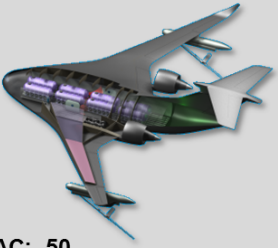



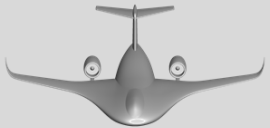
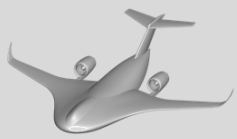
	Tanker	Airlifter	Commercial
Strategic	 <p># AC: 50 IOC: 2035</p>	 <p># AC: 270 IOC: 2035</p>	 <p># AC: 650 IOC: 2016</p>
Tactical	 <p># AC: 250 IOC: 2028</p>	 <p># AC: 325 IOC: 2030</p>	 <p># AC: 270 IOC: 2016</p>

Figure 40: HWB Market Size Assessment.

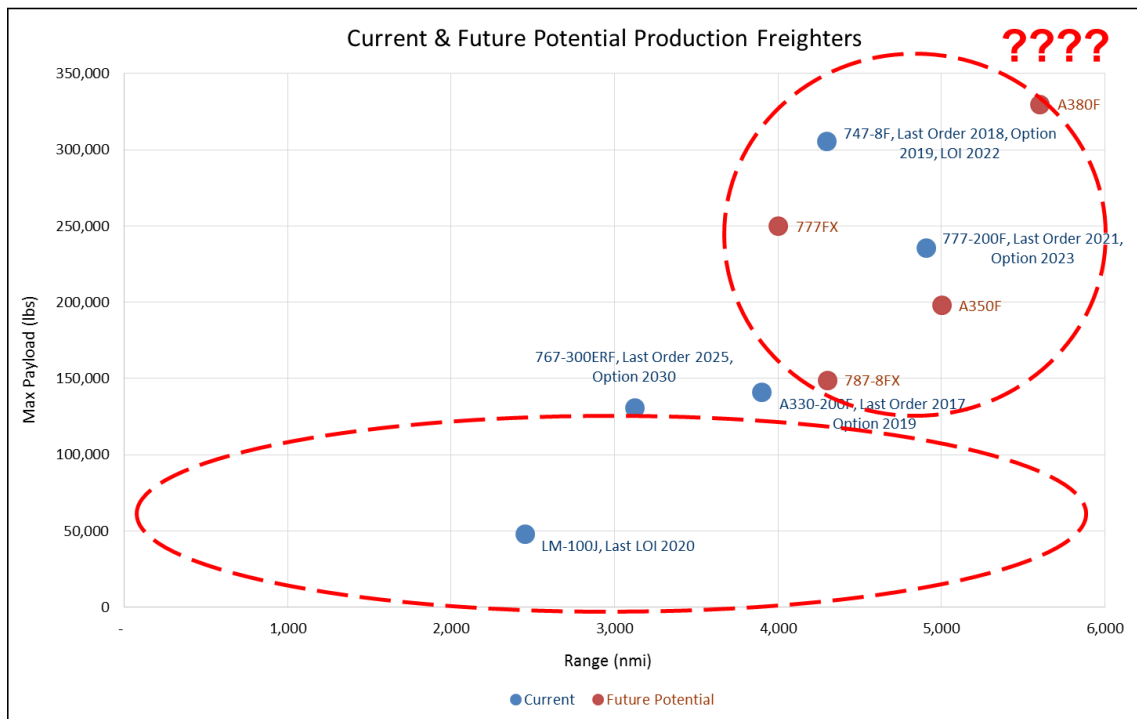
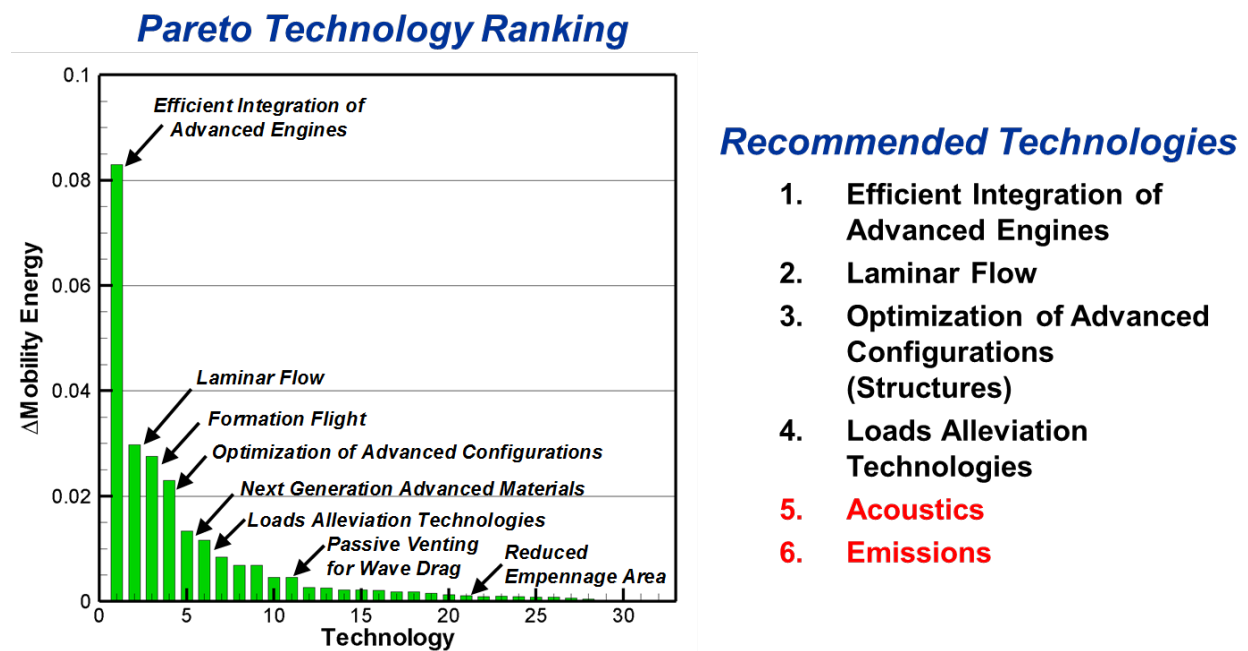


Figure 41: HWB Commercial Freighter Market Assessment.



## Technology Maturation Roadmap

This section summarizes the results from the technology maturation roadmap development documented in detail in the “AHWB Commercial Cargo Technology Maturation Roadmap Report.” This roadmap is based primarily upon previous research conducted under the AFRL sponsored RCEE program that resulted in the development of a Pareto ranking of highest pay-off fuel saving technologies. Results from this study are depicted in Figure 42. From this figure, it can be seen that the highest pay-off fuel saving technologies recommended for further maturation are: efficient integration of advanced engines, laminar flow, optimization of advanced configurations (structures), and loads alleviation technologies. Since acoustics and emissions were not a primary concern with the previous study, they were not listed in the Pareto ranking, however, they have been added to the list of recommendations.



**Figure 42: RCEE Program Based Highest Pay-Off Fuel Saving Technologies for Maturation.**

The resulting recommended technology maturation roadmap is depicted in Figure 43. From this figure, details of the individual tasking for each technology can be seen along with overall time phasing. As depicted, specific recommendations for maturation as part of the efficient integration of advanced engines technology include: powered open rotor wind tunnel testing in the NTF, low speed powered testing (potentially in the AFRL Subsonic Aerodynamic Research Laboratory) as well as distributed propulsion studies. For laminar flow, specific recommendations include CFD based simulations on the NASA sponsored Common Research Model to confirm / validate NASA results and a follow-on NTF wind tunnel test of a natural laminar flow variant of the HWB. For structural optimization, numerous optimization and design trades are recommended followed up by large scale testing. For acoustics maturation, specific recommendations include quantification of the acoustics performance of the baseline configuration and an assessment of the noise reduction

possible with advanced technologies, such as landing gear fairings. Finally, for loads alleviation technologies, specific recommendations include quantification of the impact of wing loads and landing gear alleviation technologies on the structural weight of the HWB configuration, along with an assessment of the impact of aeroelastic tailoring for performance improvements at off-design conditions.

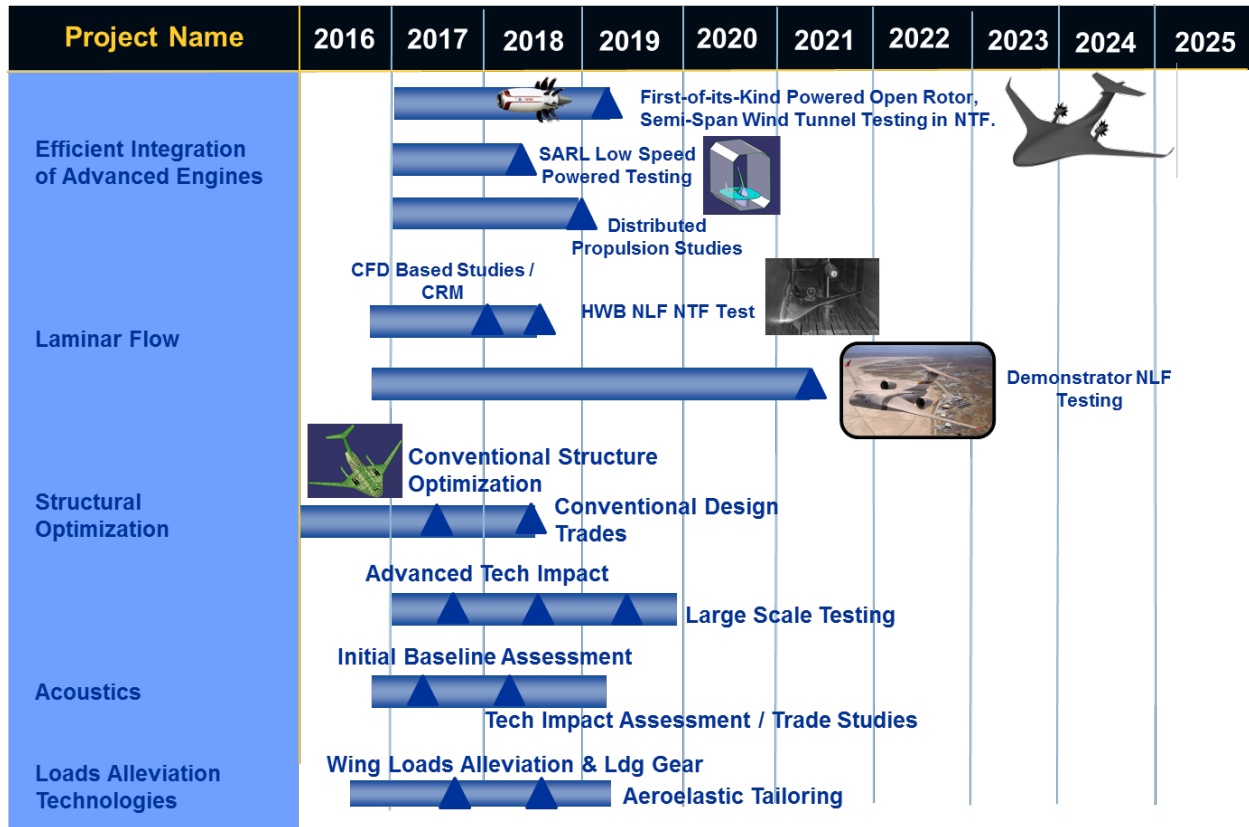


Figure 43: Recommended Technology Maturation Roadmap.

A preliminary estimate of the extent of natural laminar flow (NLF) possible on the HWB, using recently developed NASA design methods (Reference 9), is depicted in Figure 44. From this figure, it can be seen that the estimated extent of NLF ranges from 10% of the chord inboard to approximately 65% of the chord outboard. Only upper surface NLF is considered due to the need for a Krueger-like leading-edge device. Results indicate that drag savings as high as 10 to 20 drag counts can be achieved. This is in addition to the HWB performance documented in this report as no laminar flow is assumed in these results.

Mach = 0.81    Re = 44M     $\Lambda_{LE,in} \approx 57^\circ$      $\Lambda_{LE,out} \approx 35^\circ$      $N_{crit} = 13$

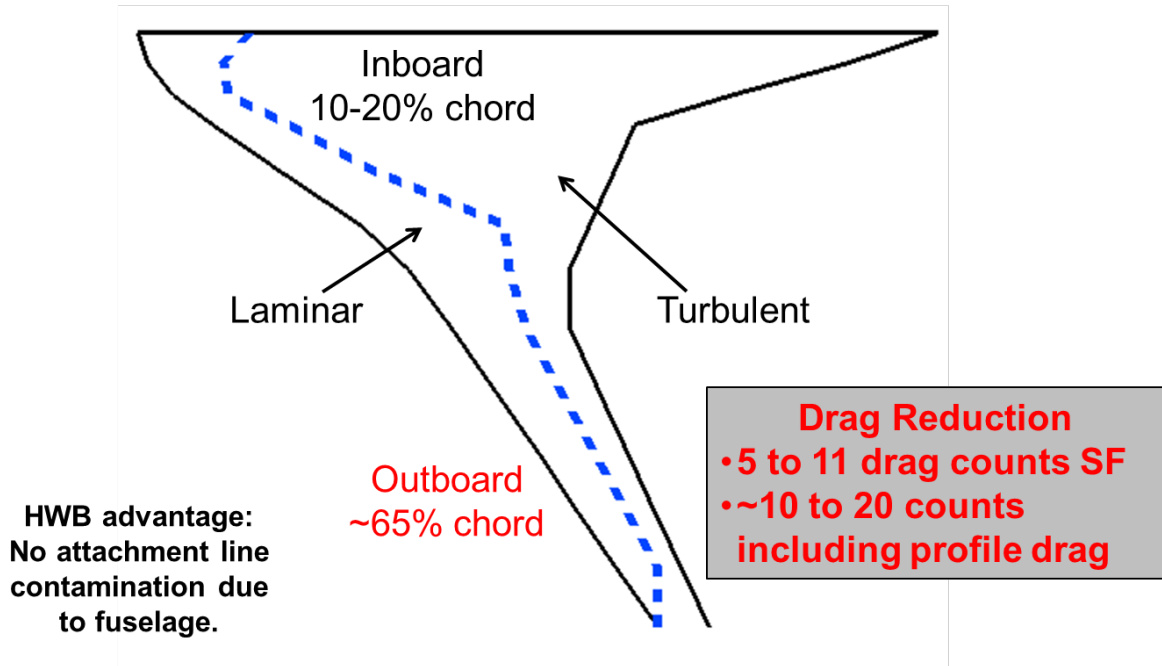


Figure 44: Estimated Extent and Benefit of Natural Laminar Flow on the HWB.

## VI. Conclusions

Results documented in this report are part of a comprehensive effort performed to assess the viability of the HWB as a commercial freighter. As part of this effort, a total of three configurations were developed, including: 1) an advanced tube-and-wing 777F sized configuration, 2) a 757 sized HWB configuration (HWB 757), and 3) a 777 sized HWB configuration (HWB). Results confirmed the scalability of the HWB concept. Detailed performance comparisons were made with today's existing freighter fleet and a comparable future fleet of the same technology level. Results documented in this report indicate that an HWB-based commercial freighter, using technology levels available at an Entry Into Service (EIS) date of 2030-2035, would use approximately 30 – 60% less fuel than today's commercial freighters and ~7% less fuel than an advanced tube-and-wing configuration using the same technology levels. These fuel saving estimates are dependent on freighter size and mission range.

## REFERENCES

1. Frink, N. T., and Pirzadeh, S. Z.; "Tetrahedral Finite-Volume Solutions to the Navier-Stokes Equations on Complex Configurations," Presented at the Tenth International Conference on Finite elements in Fluids, Tucson, AZ, January 5-8, 1998.
2. Frink, N. T.; "Assessment of an Unstructured-Grid Method for Predicting 3-D Turbulent Viscous Flows," AIAA 96-0292, January 1996.
3. Campbell, R.L., "Efficient Viscous Design of Realistic Aircraft Configurations," AIAA 1998-2539.
4. Hooker, R., Wick, A., Zeune, C., Agelastos, A., "Over Wing Nacelle Installations for Improved Energy Efficiency," AIAA Applied Aerodynamics 2013, July 2013.
5. Hooker, J. R., Wick, A., "Design of the Hybrid Wing Body for Fuel Efficient Air Mobility Operations," AIAA 2014-1285.
6. Hooker, J. R., Wick, A., Zeune, C., Jones, G., and Milholen, W., "Design and Transonic Wind Tunnel Testing of a Cruise Efficient STOL Military Transport," AIAA 2013-1100.
7. Hooker, R., Wick, A., Zeune, C., Agelastos, A., "Over Wing Nacelle Installations for Improved Energy Efficiency," AIAA Applied Aerodynamics 2013, July 2013.
8. Wick, A., Hooker, R., Walker, J., Chan, D., Plumley, R., Zeune, C., "Hybrid Wing Body Performance Validation at the National Transonic Facility," AIAA 2017-0099.
9. Campbell, R. L., Lynde, M. N., "Natural Laminar Flow Design for Wings with Moderate Sweep," AIAA 2016-4320.

**REPORT DOCUMENTATION PAGE**

Form Approved  
OMB No. 0704-0188

The public reporting burden for this collection of information is estimated to average 1 hour per response, including the time for reviewing instructions, searching existing data sources, gathering and maintaining the data needed, and completing and reviewing the collection of information. Send comments regarding this burden estimate or any other aspect of this collection of information, including suggestions for reducing the burden, to Department of Defense, Washington Headquarters Services, Directorate for Information Operations and Reports (0704-0188), 1215 Jefferson Davis Highway, Suite 1204, Arlington, VA 22202-4302. Respondents should be aware that notwithstanding any other provision of law, no person shall be subject to any penalty for failing to comply with a collection of information if it does not display a currently valid OMB control number.  
**PLEASE DO NOT RETURN YOUR FORM TO THE ABOVE ADDRESS.**

<b>1. REPORT DATE (DD-MM-YYYY)</b> 01- 07- 2017		<b>2. REPORT TYPE</b> Contractor Report		<b>3. DATES COVERED (From - To)</b>	
<b>4. TITLE AND SUBTITLE</b> Commercial Cargo Derivative Study of the Advanced Hybrid Wing Body Configuration with Over-Wing Engine Nacelles				<b>5a. CONTRACT NUMBER</b> NNL10AA06B	
				<b>5b. GRANT NUMBER</b>	
				<b>5c. PROGRAM ELEMENT NUMBER</b>	
<b>6. AUTHOR(S)</b> Hooker, John R.; Wick, Andrew T.; Hardin, Christopher J.				<b>5d. PROJECT NUMBER</b>	
				<b>5e. TASK NUMBER</b> NNL15AB18T	
				<b>5f. WORK UNIT NUMBER</b> 081876.02.07.50.06.01.01	
<b>7. PERFORMING ORGANIZATION NAME(S) AND ADDRESS(ES)</b> NASA Langley Research Center Hampton, VA 23681-2199				<b>8. PERFORMING ORGANIZATION REPORT NUMBER</b>	
<b>9. SPONSORING/MONITORING AGENCY NAME(S) AND ADDRESS(ES)</b> National Aeronautics and Space Administration Washington, DC 20546-0001				<b>10. SPONSOR/MONITOR'S ACRONYM(S)</b> NASA	
				<b>11. SPONSOR/MONITOR'S REPORT NUMBER(S)</b> NASA-CR-2017-219653	
<b>12. DISTRIBUTION/AVAILABILITY STATEMENT</b> Unclassified - Subject Category 02 Availability: NASA STI Program (757) 864-9658					
<b>13. SUPPLEMENTARY NOTES</b> Langley Technical Monitor: David T. Chan					
<b>14. ABSTRACT</b> LM has leveraged our partnership with the Air Force Research Laboratory (AFRL) and NASA on the advanced hybrid wing body (HWB) concept to develop a commercial freighter which addresses the NASA Advanced Air Transport Technology (AATT) Project goals for improved efficiency beyond 2025. The current Air Force Research Laboratory (AFRL) Revolutionary Configurations for Energy Efficiency (RCEE) program established the HWB configuration and technologies needed for military transports to achieve aerodynamic and fuel efficiencies well beyond the commercial industry's most modern designs. This study builds upon that effort to develop a baseline commercial cargo aircraft and two HWB derivative commercial cargo aircraft to quantify the benefit of the HWB and establish a <u>technology roadmap</u> for further development.					
<b>15. SUBJECT TERMS</b> Commercial freighter; Hybrid wing body; Over wing nacelle					
<b>16. SECURITY CLASSIFICATION OF:</b>			<b>17. LIMITATION OF ABSTRACT</b>	<b>18. NUMBER OF PAGES</b>	<b>19a. NAME OF RESPONSIBLE PERSON</b>
<b>a. REPORT</b>	<b>b. ABSTRACT</b>	<b>c. THIS PAGE</b>			STI Help Desk (email: help@sti.nasa.gov)
U	U	U	UU	41	<b>19b. TELEPHONE NUMBER (Include area code)</b> (757) 864-9658